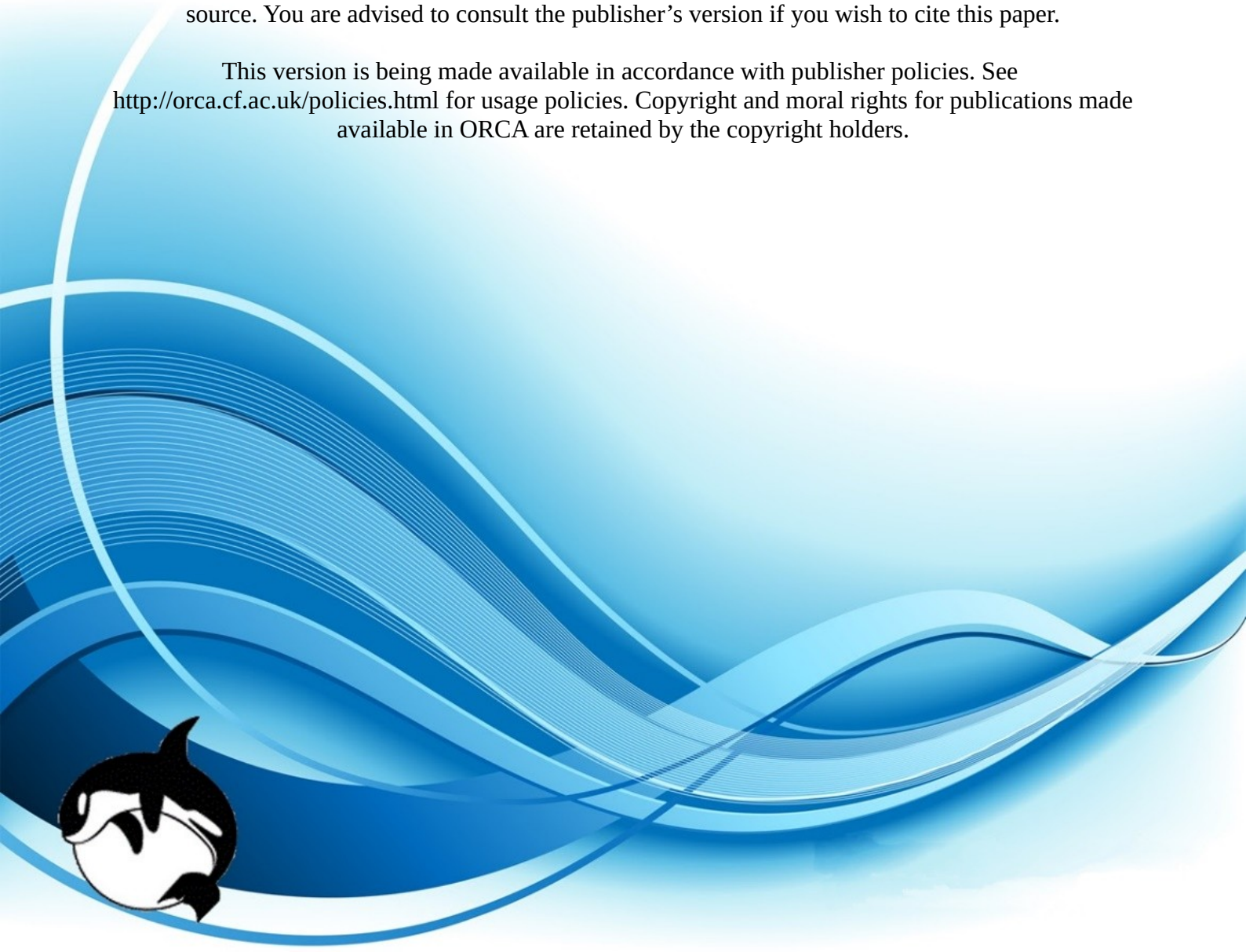

Accepted Manuscript

*Journal of the Geological Society*

# The origin(s) and geodynamic significance of Archaean ultramafic-mafic bodies in the mainland Lewisian Gneiss Complex, North Atlantic Craton

George L. Guice, Iain McDonald, Hannah S. R. Hughes, John M. MacDonald & John W. Faithfull

DOI: https://doi.org/10.1144/jgs2020-013

Received 17 January 2020
Revised 1 March 2020
Accepted 2 March 2020



Supplementary material at https://doi.org/10.6084/m9.figshare.c.4878588

To cite this article, please follow the guidance at https://www.geolsoc.org.uk/~/media/Files/GSL/shared/pdfs/Publications/AuthorInfo_Text.pdf?la=en

# The origin(s) and geodynamic significance of Archaean ultramafic-mafic bodies in the mainland Lewisian Gneiss Complex, North Atlantic Craton

George L. Guice[a,b,*]; Iain McDonald[b]; Hannah S. R. Hughes[c,d]; John M. MacDonald[e]; John W. Faithfull[f]

[a] National Museum of Natural History, Smithsonian Institution, 10th & Constitution Avenue, Washington, D.C. 20560. USA.

[b] School of Earth and Ocean Sciences, Cardiff University, Main Building, Park Place, Cardiff. CF10 3AT. UK.

[c] Camborne School of Mines, College of Engineering, Mathematics & Physical Sciences, University of Exeter, Penryn Campus, Penryn, Cornwall, TR10 9FE, UK.

[d] School of Geosciences, University of the Witwatersrand, Private Bag 3, Wits 2050, Johannesburg South Africa.

[e] School of Geographical and Earth Sciences, Gregory Building, University of Glasgow, Glasgow, G12 8QQ

[f] Hunterian Museum, University of Glasgow, University Avenue, Glasgow, G12 8QQ

*corresponding author: GuiceG@si.edu



**Keywords:** Archaean geodynamics; Archean; cratonisation; North Atlantic Craton; Lewisian; PGE; granulite; layered intrusion; mantle

**ABSTRACT**

The geodynamic regime(s) that predominated during the Archaean remains controversial, with the plethora of competing models largely informed by felsic lithologies. Ultramafic-mafic rocks displaying distinctive geochemical signatures are formed in a range of Phanerozoic geotectonic environments. These rocks have high melting points, making them potentially useful tools for investigating Archaean geodynamic processes in highly metamorphosed regions. We present field mapping, petrography, traditional bulk-rock geochemistry, and platinum-group element geochemistry for 12 ultramafic-mafic bodies in the Lewisian Gneiss Complex (LGC), which is a highly metamorphosed fragment of the North Atlantic Craton in northwest Scotland. Our data indicate that most of these occurrences are layered intrusions emplaced into the tonalite-trondhjemite-granodiorite (TTG)-dominated crust prior to polyphase metamorphism, representing a significant re-evaluation of the LGC's magmatic evolution. Of the others, two remain ambiguous, but one (Loch an Daimh Mor) has some geochemical affinity with abyssal/orogenic peridotites and may represent a fragment of Archaean mantle, although further investigation is required. The ultramafic-mafic bodies in the LGC thus represent more than one type of event/process. Compared with the TTG host rocks, these lithologies may preserve evidence of protolith origin(s), with potential to illuminate tectonic setting(s) and geodynamic regimes of the early Earth.

## INTRODUCTION

Plate tectonics is the unifying theory of modern geological knowledge, providing a framework for the interpretation of Earth's Phanerozoic geology. However, the nature and timing of its onset remains a matter of considerable debate (Arndt, 2013; Cawood et al., 2018; Kamber, 2015), leading to the proposal of a plethora of competing geodynamic models to explain the Archaean Earth (e.g., Bédard, 2018; Bédard et al., 2013; Brown and Johnson, 2018; Johnson et al., 2019, 2017; Kamber, 2015; Van Kranendonk et al., 2004). Recently, in an attempt to pinpoint a date for the onset of plate tectonics, authors have assessed the temporal variation of a variety of geological and geochemical proxies. Such proxies include: (i) the presence/absence of passive margins and paired metamorphic belts (Brown and Johnson, 2018; Cawood et al., 2018); (ii) various element ratios recorded by the bulk-rock geochemical composition of granitoid (Halla, 2018; Johnson et al., 2019) and/or mafic rocks (Condie, 2018; Dhuime et al., 2015; Moyen and Laurent, 2018; Smithies et al., 2018); and (iii) the apparent thermal gradients (*T/P*) of peak metamorphism (Brown and Johnson, 2018). This global approach has been successful in identifying a significant evolution in Earth's behaviour between ~3.3 Ga and ~2.5 Ga, with such evolution perhaps pertaining to the onset of Earth's current geodynamic regime (see Cawood et al. 2018). However, this approach does not provide material evidence of the specific geodynamic processes that operated throughout the Archaean Eon. Part of the challenge, when studying rocks of this age, is the likelihood for primary signatures to be overprinted by metamorphism and associated processes, such as partial melting and metasomatism.

On the modern Earth, ultramafic-mafic rocks are both formed and preserved in a variety of geodynamic environments, displaying distinctive geological associations and geochemical signatures. For example, the residual mantle portion of an ophiolite exhibits significant trace element depletion (Godard et al., 2008; Paulick et al., 2006) relative to mantle derived melts that may crystallise as komatiites or the ultramafic-mafic portions of a layered intrusion (Furnes et al., 2012). Moreover, when compared to felsic lithologies, the constituent minerals of ultramafic rocks have high melting

temperatures, making them relatively resilient to the subsequent effects of high-temperature metamorphism and associated partial melting (Bowen, 1956). Therefore, if the effects of alteration and associated metasomatism, which are often cryptic, can be constrained (Guice, 2019; Guice et al., 2019, 2018b), ultramafic-mafic rocks have the potential to establish the physical manifestations of Archaean geodynamic processes. Specifically, confident identification of residual mantle rocks associated with age equivalent intrusions and submarine lavas (as part of an ophiolite that displays structural and lithological relationships comparable to Phanerozoic examples) would represent extremely strong evidence in favour of plate tectonics having operated (Bédard et al., 2013; Kamber, 2015; Rollinson, 2007). Presently, suggested Archaean ophiolite occurrences remain highly contested, with the proposed examples often not withstanding detailed examination (Guice et al., 2019; Szilas et al., 2018, 2015).

The ultramafic-mafic complexes of the mainland Lewisian Gneiss Complex (LGC) – a classic and intensely studied portion of Archaean crust located in NW Scotland – have been interpreted as representing mafic magmatism in settings that reflect different Archaean geodynamic regimes. Such interpretations include: (i) remnants of an early, possibly oceanic, mafic-ultramafic crust (Sills, 1981); (ii) fragments of one or more layered intrusions emplaced into existing crust (Bowes et al., 1964; Guice et al., 2018a); (iii) accreted oceanic crust (Park and Tarney, 1987); or (iv) the sagducted remnants of one or more greenstone belt(s) (Johnson et al., 2016). In a recent study, which utilised detailed field mapping, petrography and spinel mineral chemistry, Guice et al. (2018a) interpreted the Ben Strome Complex as representing a layered intrusion emplaced into the tonalite-trondhjemite-granodiorite (TTG)-dominated crust prior to granulite-facies metamorphism at ~2.7 Ga. This interpretation of the Ben Strome Complex, which represents the largest (7 $km^2$) and best exposed ultramafic-mafic complex in the mainland LGC, is counter to the bulk of previous literature, which, based on the seemingly dispersed nature of the ultramafic-mafic rocks (e.g., Park et al., 2002) and an apparent (but contested; Guice et al., 2018a; Johnson et al., 2016) cross-cutting relationship at Geodh' nan Sgadan (Rollinson and Windley, 1980; Fig. 1), assumes that these lithologies pre-date

the TTG protoliths. If this interpretation withstands further interrogation and is extended to other ultramafic-mafic complexes in the region, it requires a significant re-evaluation of the magmatic evolution of the LGC. Moreover, multiple studies have suggested that the ultramafic-mafic rocks of the mainland LGC may reflect more than one origin (Guice et al., 2018a; Rollinson and Gravestock, 2012), potentially recording multiple phases of temporally and/or petrogenetically distinct phases of Archaean ultramafic-mafic magmatism, including the potential incorporation of Archaean mantle fragments.

In this paper, we present field mapping and observations, petrography, major and trace element bulk-rock geochemistry, and, for the first time, platinum-group-element (PGE) bulk-rock geochemistry for 12 ultramafic-mafic complexes in the mainland LGC. The spatial distribution of the ultramafic-mafic complexes is detailed in Figure 1. Using the presented data, we aim to:

(i) Examine the validity of the layered intrusion hypothesis ("Ben Strome model") for other ultramafic-mafic complexes in the mainland LGC;

(ii) If/where this hypothesis fails, assess the possibility that fragments of Archaean mantle may be preserved within this portion of the North Atlantic Craton.

## REGIONAL GEOLOGY

The mainland LGC crops out as a 125 x 20 km coastal strip located in northwest Scotland, west of the Moine Thrust (Peach et al., 1907; Sutton and Watson, 1951; Wheeler et al., 2010). Partially covered by Neoproterozoic to Ordovician sedimentary rocks, the mainland LGC is dominated by amphibolite- to granulite-facies TTG gneiss and has experienced a protracted and complex history of magmatism, metamorphism and deformation (Peach et al., 1907; Wheeler et al., 2010). Volumetrically subordinate ultramafic, mafic and metasedimentary rocks accompany the TTG gneiss, with all these lithologies cross-cut by a suite of Palaeoproterozoic mafic dykes (the "Scourie Dykes") and later pegmatitic sheets in some areas (Park et al., 2002). Traditionally, the mainland LGC has been subdivided into a granulite-facies Central Region and amphibolite-facies Northern and Southern

Regions (Fig. 1). Relative to the hornblende-bearing Northern and Southern Regions, the pyroxene-bearing Central Region is depleted in Cs, Rb, U, Th, K and Ta (Sheraton et al., 1973), with the latter interpreted as representing deeper crustal levels than the former (Park and Tarney, 1987). More recently, geochronological-based studies, which utilise U-Pb dating of zircon in TTG gneiss, have shown that the mainland LGC records a wide range of protolith ages and metamorphic histories (Friend and Kinny, 2001; Kinny et al., 2005; Kinny and Friend, 1997; Love et al., 2010, 2004), with the mainland LGC therefore interpreted to represent up to six "terranes". Although the precise number of terranes remains controversial (Park, 2005), the Laxford Shear Zone (see Fig. 1) is generally accepted as a significant crustal boundary (Goodenough et al., 2013, 2010).

Although many aspects of the magmatic and metamorphic evolution remains the topic of considerable discussion, it is generally accepted that the magmatic precursors to the TTG gneiss crystallised between 3.1 and 2.7 Ga (Friend and Kinny, 2001; Kinny et al., 2005; Love et al., 2010; MacDonald et al., 2015; Whitehouse and Kemp, 2010). A widespread granulite-facies tectonothermal event – known locally as the Badcallian – most likely occurred between 2.8 and 2.7 Ga, with peak *P-T* conditions estimated at 0.8-1.2 GPa and > 900°C (Andersen et al., 1997; Barnicoat, 1983; Barnicoat and O'Hara, 1978; Barooah and Bowes, 2009; Cartwright et al., 1985; Corfu, 1998; Corfu et al., 1994; Crowley et al., 2015; Evans and Lambert, 1974; Feisel et al., 2018). This event, which is characterised by a pervasive, shallow- to moderate-dipping gneissosity that displays open to isoclinal folds (Guice et al., 2018a; Park et al., 2002), likely led to partial melting of the TTG gneisses and some mafic lithologies (Johnson et al., 2013, 2012). The Badcallian was succeeded by a granulite- to amphibolite-facies tectonothermal event – known locally as the Inverian – between c. 2.5 and 2.4 Ga (Beach, 1974, 1973; Corfu et al., 1994; Whitehouse and Kemp, 2010). This event, which is poorly constrained due to subsequent reactivation, is defined as preceding the 2.42-2.38 Ga emplacement of the NW-SE-trending Scourie Dykes (Davies and Heaman, 2014; Heaman and Tarney, 1989). These steeply-dipping dykes can be up to 100 m wide, with the NW-SE trend likely controlled by pre-existing shear zones (Weaver and Tarney, 1981). Finally, a greenschist- to amphibolite-facies

tectonothermal event(s) – known locally as the Laxfordian – occurred between c. 1.9 and 1.6 Ga, forming E-W-trending shear zones that are typically tens of metres wide and characterised by a thinning of the Badcallian foliation, and, especially north of the Laxford shear zone, granite emplacement (Beach, 1974; Beach et al., 1974; Goodenough et al., 2013, 2010).

## FIELD RELATIONSHIPS

With the exception of the Loch an Daimh Mor and Geodh' nan Sgadan Complexes, the studied ultramafic-mafic complexes (namely: Achiltibuie, Achmelvich, Ben Auskaird, Ben Strome, Drumbeg, Loch Eilean na Craoibhe Moire, North Scourie Bay and Scouriemore) share several characteristics. Exposed across areas up to 7 $km^2$, these complexes are composed of modally layered ultramafic and mafic rocks (Fig. 2). This layering is extremely striking in the ultramafic rocks (Fig. 3a-c), but, as a consequence of the greater susceptibility to metamorphism (i.e., partial melting), is more discrete in the mafic rocks (Fig. 3d). There is a consistent parallelism between the gneissose foliation in the surrounding TTG, layering in the ultramafic-mafic rocks, and all lithological contacts (Fig. 2), as described by previous studies (Bowes et al., 1964; Guice et al., 2018a; Johnson et al., 2016). The ultramafic portions comprise dominant metapyroxenite (metawebsterite and metaolivine-websterite) and rare metaperidotite (metalherzolite), while the mafic portions contain metagabbro, garnet-metagabbro, garnet-amphibolite and amphibolite in variable proportions. The contacts between the complexes and surrounding TTG gneiss are tectonic where observed, but actual exposures are remarkably scarce. Similarly, although many of the contacts between ultramafic and mafic units are also rare, those observed are gradational on a scale of tens of centimetres (Guice et al., 2018a).

Individual ultramafic units can be traced for hundreds of metres along strike and are mostly several metres to several tens of metres in apparent thickness (Fig. 2a-b). The metawebsterites within these ultramafic portions have distinctly grey weathered surfaces and generally show little-to-no internal layering, while the grey-brown metaolivine-websterites and brown metaperidotites exhibit

prominent internal layering (Fig. 3a-c). The metaolivine-websterite and metaperidotite layers are generally negatively weathered relative to the pyroxenitic layers. Moreover, the ultramafic rocks in all of these complexes consistently exhibit gradational and sharp contacts between individual layers; gradational variation in modal mineral abundances within individual layers; and truncation of layers on the centimetre-scale (Fig. 3a-c). The mafic portions of these complexes comprise garnet-metagabbro, metagabbro, garnet-amphibolite and amphibolite in varying proportions. In places, the mafic rocks show centimetre- to metre-scale layering that is more discrete than in the ultramafic rocks, with individual layers defined by the proportions of garnet, pyroxene and plagioclase (Fig. 3d). Garnet, which commonly occurs on the centimetre-scale and often exhibits retrogressive plagioclase and/or amphibole rims, may form large clots up to 1 m in diameter. Millimetre- to centimetre-scale horizons containing high proportions of oxide minerals (dominantly magnetite and ilmenite) occur rarely (e.g., at Ben Strome; NC 25716/36120).

While sharing the salient features outlined above, these complexes also exhibit some variation in structural architecture (Fig. 2). For example, Ben Strome (Guice et al., 2018a) and Drumbeg (Fig. 2b) display Badcallian to Inverian folds that are cross-cut by Laxfordian shear zones and/ or Scourie Dykes. In contrast, the steeply-dipping (70-90°) Loch Eilean na Craoibhe Moire exhibits a NW-SE, Inverian/ Laxfordian trend that is cross-cut by Scourie Dykes and a suite of NE-SW-trending, likely Phanerozoic, faults (Fig. 2a). This variation can probably be attributed to the close proximity of the Loch Eilean na Craoibhe Moire Complex to the Laxford Shear Zone (Fig. 1), while the Ben Strome and Drumbeg Complexes are located further south. Moreover, while the ultramafic and mafic rocks occur, on average, in a 1:2 ratio, significant variation is observed between occurrences. The Loch Eilean na Craoibhe Moire and Drumbeg Complexes comprise more than 50 % ultramafic rocks, while the Ben Auskaird Complex contains 100 % mafic rocks. This variation is unlikely a function of the outcrop availability, as all the complexes are well-exposed.

In contrast to this group of complexes, the Loch an Daimh Mor Complex – located in the NW of the Central Region (Fig. 1) – is represented by a 500 $m^2$ area containing several irregularly-shaped pods predominantly comprising ultramafic rocks (Fig. 2c). The generally massive ultramafic rocks, which are almost exclusively metaperidotite, are highly serpentinised (± talc), exhibit grey-brown weathered surfaces (Fig. 3e) and show mm-scale chromite in places. Metaperidotite is variably veined by separate carbonate- and orthopyroxene-rich veins, with the latter more numerous than the former (Faithfull et al., 2018). The orthopyroxene-dominated veins, which display sharp contacts with the surrounding ultramafic rocks, are 1-40 cm thick and contain centimetre-scale zircon crystals interpreted as associated with Inverian metasomatism (Faithfull et al., 2018). Adjacent metagabbro-dominated mafic rocks, which occur in association with intermediate gneiss, are poorly-exposed and locally contain coarse garnet. Importantly, the foliation in the surrounding TTG gneiss displays distinctive discordance with the lithological contacts on the map-scale (Fig. 2c).

In contrast to all previously described occurrences, the Geodh' nan Sgadan Complex – located less than 2 km SW of Loch an Daimh Mor (Fig. 1) – is a moderately-dipping, 15 m thick package of layered mafic rocks (Guice et al., 2018a; Fig. 2f). The Complex is underlain and overlain by TTG gneiss, with the gneissosity in the TTG parallel to the layering in the mafic rocks. Ultramafic rocks are absent, and the surrounding TTG gneiss contains a large number of centimetre-scale mafic pods that are possibly derived from the layered body. Layering in the plagioclase-rich mafic rocks is defined by millimetre-scale variation in the modal abundance of plagioclase, amphibole and pyroxene, with garnet restricted to rare, centimetre-scale horizons (Guice et al., 2018a). Such layering ranges from well-defined and laterally continuous on a scale of tens of metres to poorly-defined and chaotic (Fig. 3f).

## ANALYTICAL INSTRUMENTATION AND METHODOLOGY

### *Bulk-rock geochemistry*

All analysed samples were crushed and ground to a fine powder using the rock preparation facilities at Cardiff University (School of Earth and Ocean Sciences). Weathered surfaces were removed using a diamond-bladed rock saw, before samples were crushed using a Mn-steel jaw-crusher and ground using an agate ball mill. Powdered samples were then ignited (at ~900°C) for 2 hours, with LOI determined gravimetrically.

#### *Lithophile elements*

A sample mass of 0.1 g was accurately weighed and mixed with 0.6 g of Li metaborate flux in a Claisse BIS! Pt-Rh crucible (see McDonald and Viljoen 2006 for full details). Approximately 0.5 mL of a Li iodide solution was added as a non-wetting agent, before the mixture was fused over a propane burner on a Claisse FLUXY (automated) fusion system. The mixture was subsequently poured into a Teflon beaker containing 50 ml of 4 % $HNO_3$, where it was dissolved using a magnetic stirrer. Following dissolution of all glass fragments, the solution was spiked with 1 mL of a 100 ppm Rh spike solution (for use an as internal standard) and made up to 100 mL with 18.2 MΩ deionised water (McDonald and Viljoen, 2006). Samples were subsequently analysed for major and trace elements using ICP-OES and ICP-MS respectively.

Standard reference materials and blanks were prepared and analysed using the methodology and instrumentation described above, with the sample material omitted for the blanks. Accuracy was constrained by analysis of a suite of international standard reference materials (see supplementary material). Precision was constrained by duplicate analyses of ~5 % of samples and by conducting repeat analyses of standards in different sample batches.

*Platinum-group elements and gold*

Samples were prepared by Ni sulphide fire assay and Te co-precipitation (fully described in: Huber et al. 2001, McDonald and Viljoen 2006). Typically, 10 g of sample material (as ground rock powder; method described above) is mixed with: 5 g of silica, 6 g of Na-carbonate, 12 g of borax, 0.9 g of sulphur and 1.1 g of carbonyl-purified Ni. Reagents were thoroughly mixed before samples were transferred to fire-clay crucibles before being fired at 1050°C for 90 minutes. Buttons were dissolved using concentrated HCl, with co-precipitation achieved using Te and $SnCl_2$. The filtered residues were digested using 3 ml of concentrated $HNO_3$ and 4 ml of concentrated HCl in sealed 15 ml Saville screw-top Teflon vials. After the residue had dissolved, the liquid contents were transferred to 50 ml volumetric flasks, spiked with a 2.5 ppm Tl spike (for use as an internal standard) and made up to 50 ml with 18.2 MΩ deionised water. Solutions were then analysed for PGE and Au using an ICP-MS system at Cardiff University.

Standard reference materials and blanks were prepared and analysed using the methodology and instrumentation described above, with the sample material omitted for the blanks, for which a 10 g Si mass was used. Accuracy was constrained by analysis of a suite of international standard reference materials (see supplementary material). Precision was constrained by conducting duplicate analyses of ~10 % of samples, and by conducting repeat analyses of standards in different sample batches.

***Element mapping***

Detailed petrographic assessment by element mapping used a Zeiss Sigma HD Field Emission Gun A-SEM (A-SEM) equipped with two Oxford Instruments 150 mm2 Energy Dispersive X-ray Spectrometry (EDS) detectors at the School of Earth and Ocean Sciences, Cardiff University. Operating conditions were set at 20 kV and aperture size to 120 µm, with a nominal beam current of 4 nA and working distance of 8.9 mm. Using Aztec software, maps were acquired at 100 to 150× magnifications, with resulting pixel sizes ranging from 10 to 22 µm, depending on the resolution of acquired spectral

images. A process time of 1 µs was used in conjunction with a pixel dwell time of 3000–6000 µs. Element maps were then background correlated and element overlaps deconvolved using Aztec software, before modal mineralogy was calculated from relative element concentrations using the analyse phases algorithm in Aztec. Boundary tolerance and grouping level were set at 2 and 1 respectively, with any unassigned pixels (typically < 5 %) discarded from the modal mineralogy.

## PETROGRAPHY

A total of 62 polished thin sections (including 37 ultramafic samples and 25 mafic samples) from the 12 studied complexes were made at Cardiff University and subject to petrographic assessment. Further to basic optical microscopy, 33 samples were subject to detailed petrographic assessment by element mapping using an A-SEM. Where possible, these maps were utilised to estimate modal mineral proportions, with details of the instrumentation and methodology utilised described above. The location (GPS coordinates in British National Grid) and modal mineral proportion of each sample is included in Table 1 (ultramafic rocks) and Table 2 (mafic rocks). These tables also detail both the average and range of modal mineral proportions for each ultramafic-mafic complex, with the sections below summarising the broader petrographic features observed in the ultramafic and mafic lithologies studied.

### *Ultramafic rocks*

The modal mineral proportions of the ultramafic rocks assessed vary between and within complexes (Table 1), but the samples exhibit several consistent mineralogical and textural features (Fig. 4a-c). In terms of basic mineralogy, the ultramafic rocks comprise (in variable proportions): olivine, serpentine, orthopyroxene, clinopyroxene, amphibole, spinel and accessory sulphide phases (Table 1). Olivine is rarely preserved as millimetre-scale, subhedral grains or remnants within masses of fine-grained serpentine (± magnetite). Clino- and ortho-pyroxene, which are euhedral and 0.5 to 3.5 mm in diameter, are variably replaced by fine-grained (< 0.2 mm diameter) amphibole, with

orthopyroxene dominant over clinopyroxene. Late retrogressive amphibolitisation of pyroxene ranges from near-absent (occurring as rare rims on individual pyroxene grains; to near-complete within individual thin sections). Older, high-grade metamorphic pargasitic, amphibole (pale green in thin sections) occurs as < 2.1 mm diameter, generally subhedral grains, with these grains forming 120° triple junctions. Spinel occurs as euhedral to subhedral grains < 3.5 mm in diameter, while pentlandite, pyrrhotite and chalcopyrite occur rarely, as anhedral to euhedral grains < 0.2 mm diameter.

***Mafic rocks***

The mafic rocks from the Ben Strome, Ben Auskaird and Gorm Chnoc Complexes are mineralogically and texturally comparable (Table 2), while the Geodh' nan Sgadan Complex is texturally distinct (Fig. 4d-f). In the Ben Strome, Ben Auskaird and Gorm Chnoc Complexes (Fig. 4d-e), pyroxene is subhedral to anhedral, 0.5 to 2.5 mm in diameter, and variably replaced by fine-grained (< 0.2 mm diameter) amphibole, with clinopyroxene dominant over orthopyroxene. Amphibole (clear in thin section) also occurs as 0.2 to 2 mm diameter grains that commonly display pleochroism and 120° triple junctions. Garnet occurs as millimetre- to centimetre-scale, anhedral to subhedral grains that exhibit significant retrogression to plagioclase (± amphibole), commonly as rims. Magnetite is the dominant oxide phase, forming subhedral grains < 0.3 mm in diameter. Ilmenite is rare, but where present comprise < 7 % of individual samples (Table 2).

As described by Guice et al. (2018a), pyroxene in the Geodh' nan Sgadan Complex is generally 0.2 to 0.6 mm in diameter and subhedral to euhedral (fig. 4f). Pyroxene exhibits alteration to amphibole, which forms a fine-grained groundmass in most samples. Amphibole also exists as 0.2 to 0.5 mm diameter subhedral grains that display 120° triple junctions. Plagioclase feldspar is 0.4 to 0.6 mm in diameter and subhedral, with rare triple junctions and some amphibole replacement.

## BULK-ROCK GEOCHEMISTRY

From the 12 studied ultramafic-mafic complexes, a total of 45 ultramafic and 27 mafic rocks were analysed for bulk-rock major and trace element geochemistry, with a smaller sample set analysed for PGE and Au (44 ultramafic and 6 mafic samples). Details of the analytical instrumentation and methodology are described above, with the precision calculations, analyses of standard reference material, and raw data included in the supplementary material.

Table 3 summarises the geochemical characteristics of each complex by outlining the range of key major element abundances, trace element ratios and PGE ratios. In-line with the aims of this paper, Figures 5-8 include comparisons with: (a) the Ben Strome ultramafic rocks considered by Guice et al. (2018b) to most closely resemble primary compositions; (b) the Ben Strome mafic rocks presented here; and (c) abyssal peridotites and ultramafic mantle rocks (data from: Godard et al., 2008, 2000; Paulick et al., 2006). Given the distinctive field characteristics shown by the Loch an Daimh Mor and Geodh' nan Sgadan Complexes, these occurrences are distinguished in Figure 5, while each complex is considered separately in Figures 6-8.

### *Major and minor elements*

As detailed fully in Table 3, the analysed ultramafic rocks contain 17 to 42 wt. % MgO, up to 0.9 wt. % $TiO_2$ and 2 to 4 wt. % $Al_2O_3$, while the mafic rocks contain 3 to 21 wt. % MgO, less than 3 % $TiO_2$ and 8 to 20 wt. % $Al_2O_3$.

As shown on bulk-rock bivariate plots, MgO in the ultramafic rocks exhibits moderate to strong negative correlations ($R^2$ = > 0.4) with $TiO_2$, $Al_2O_3$ and CaO, weak negative correlations ($R^2$ = 0.1 – 0.4) with $Na_2O$, a weak positive correlation with NiO and no correlation with $SiO_2$, $Cr_2O_3$ and $Fe_2O_3$ (Table 3; Fig. 5). With the exception of the Loch an Daimh Mor Complex, the ultramafic rocks from all other complexes show consistent overlap with the field for Ben Strome Complex ultramafic rocks (Table 3; Fig. 5). Relative to this group, the Loch an Daimh Mor Complex exhibits $SiO_2$ and NiO enrichment,

alongside $Cr_2O_3$, $Fe_2O_3$ $Al_2O_3$ and CaO depletion (Table 3; Fig. 5). These samples show partial overlap with the field for ophiolites and abyssal peridotites on MgO versus $SiO_2$, $Fe_2O_3$, CaO, $Na_2O$, NiO and $Cr_2O_3$ plots (Fig. 5), while the majority of the ultramafic rocks show no overlap with this field.

Distinctive compositional trends are not present within the mafic samples, but these rocks form a part of linear trends when considering both ultramafic and mafic lithologies. MgO displays a moderate to strong negative correlation ($R^2$ = > 0.4) with $Al_2O_3$, CaO and $Na_2O$, a weak negative correlation ($R^2$ = 0.1 – 0.4) with $SiO_2$ and $Fe_2O_3$, a moderate positive correlation with $Cr_2O_3$, and a weak positive correlation with NiO (Fig. 5). The analysed mafic rocks from the Ben Auskaird, Drumbeg, Geodh' nan Sgadan and Gorm Chnoc Complexes generally overlap with the Ben Strome field, although the Geodh' nan Sgadan and Gorm Chnoc Complexes show minor relative depletion in $TiO_2$ and $Fe_2O_2$ (Fig. 5).

### *Trace elements*

#### *Ultramafic rocks*

On chondrite-normalised REE plots (Fig. 6), the ultramafic rocks from the Ben Strome Complex considered to most closely resemble primary compositions (Guice et al., 2018b) exhibit flat overall patterns ($[La/Lu]_N$ = 0.5 – 2), with chondrite-normalised REE abundances ranging from 1.1 to 8.1. Similarly flat REE patterns are shown by the majority of ultramafic rocks from the Achiltibuie ($[La/Lu]_N$ = 0.7 – 2.3), Drumbeg ($[La/Lu]_N$ = 0.6 – 1.9), Gorm Chnoc ($[La/Lu]_N$ = 1.8 – 2.1), Loch Eilean na Craoibhe Moire ($[La/Lu]_N$ = 1.0 – 2.9), North Scourie Bay ($[La/Lu]_N$ = 2.7) and Scouriemore ($[La/Lu]_N$ = 0.8 – 5) Complexes, with these rocks showing near-complete overlap with the Ben Strome Complex ultramafic rocks (Table 3; Fig. 6). Other complexes exhibit REE patterns that can be distinguished from those of the Ben Strome rocks. The Achmelvich Complex samples exhibit positively sloping LREE ($[La/Sm]_N$ = 0.3 – 0.5), with relatively flat MREE and HREE that overlap with the Ben Strome field (Fig. 6b). The Ben Dreavie samples show significant LREE enrichment ($[La/Sm]_N$ = 6.1 – 9.7), but overlap with the Ben Strome Complex in terms of MREE and HREE (Fig. 6d). The Loch

an Daimh Mor Complex is the most distinctive, exhibiting mild depletion in MREE and HREE relative to the Ben Strome Complex (0.8 to 2.9 x chondrite), alongside negatively sloping LREE ($[La/Sm]_N$ = 1.5 – 3.2). All complexes show significant enrichment of all REE relative to the field for ophiolites and oceanic peridotites (Fig. 6).

On primitive mantle-normalised trace element plots (Fig. 7), the ultramafic rocks from the Ben Strome Complex generally show flat overall patterns ($[Nb/Yb]_N$ = 0.4 – 3.9) with no negative Nb-Ta anomalies and normalised trace element abundances between 0.2 and 15. Similarly flat trace element patterns are shown by the majority of ultramafic rocks from the Achiltibuie ($[Nb/Yb]_N$ = 0.8 – 2.6), Achmelvich ($[Nb/Yb]_N$ = 0.4 – 2.5), Drumbeg ($[Nb/Yb]_N$ = 0.6 – 1.2), Loch Eilean na Craoibhe Moire ($[Nb/Yb]_N$ = 0.4 – 2.9), North Scourie Bay ($[Nb/Yb]_N$ = 1.2) and Scouriemore ($[Nb/Yb]_N$ = 0.6 – 2.2) Complexes, with near-complete overlap with the Ben Strome field. The Ben Dreavie Complex (Fig. 7d) exhibits significant enrichment in Ba, La, Ce, Sr, Nd and Sm ($[La/Ta]_N$ = 6 – 32) relative to this field, alongside associated negative Nb-Ta-Zr-Hf-Ti anomalies. Such patterns are comparable to those Ben Strome ultramafic rocks considered by Guice et al. (2018b) to have experienced LREE enrichment by metasomatism associated with $H_2O/CO_2$-rich fluids during amphibolitisation. The Gorm Chnoc Complex ultramafic rocks (Fig. 7h) also display negative Nb-Ta-Zr-Hf anomalies ($[Nb/Yb]_N$ = 0.5 – 0.6; $[La/Ta]_N$ = 2.8 – 3.2), but, in comparison to Ben Dreavie, are lacking the associated enrichment of the LREE and elements more typically considered fluid mobile (e.g., Ba). The Loch an Daimh Mor Complex ultramafic rocks (Fig. 7i) exhibit overall flat patterns ($[Nb/Yb]_N$ = 0.5 – 2.2) and positive LREE anomalies ($[La/Ta]_N$ = 0.2 to 0.9), with mild depletion in the most incompatible (Rb to Nb) and compatible (Ti to Lu) elements.

*Mafic rocks*

On chondrite-normalised REE plots (Fig. 6), the mafic rocks from the Ben Strome Complex exhibit chondrite-normalised values between 4 and 62, with some mildly positive slopes and some mildly negative slopes ($[La/Lu]_N$ = 0.3 – 8). The Ben Auskaird mafic rocks (Fig. 6c) show minor enrichment in

the HREE and MREE relative to Ben Strome, but otherwise exhibit similar, positively sloping patterns ($[La/Sm]_N$ = 1.3 – 2.5; $[La/Lu]_N$ = 2.0 – 3.1). The one Drumbeg Complex sample shows a positively sloping pattern ($[La/Sm]_N$ = 1.5; $[La/Lu]_N$ = 7), alongside mild enrichment in almost all REE. The two samples from the Gorm Chnoc Complex (Fig. 6h) show flat MREE and HREE patterns, negatively sloping LREE ($[La/Sm]_N$ = 0.6 – 0.8; $[La/Lu]_N$ = 0.6 – 0.9) and mild depletion in all REE relative to the Ben Strome Complex. The Geodh' nan Sgadan Complex samples show the greatest distinction from the Ben Strome Complex, showing a broad range in REE contents (2 to 126 x chondrite). These rocks exhibit relatively flat MREE and HREE, alongside negatively sloping LREE ($[La/Sm]_N$ = 1.7 – 2.8).

On primitive mantle-normalised trace element plots (Fig. 7), the mafic rocks from the Ben Strome Complex generally exhibit flat patterns ($[Nb/Yb]_N$ = 0.3 – 1.9) that are punctuated by mild negative Th-U-Zr-Hf anomalies and mild positive Rb-Ba-Sr anomalies. The Ben Auskaird mafic rocks display a comparable pattern ($[Nb/Yb]_N$ = 2.2), but with a negative Sr anomaly and mild enrichment in some of the most incompatible (Ba, Th) and compatible (Tb to Lu) elements. Similarly, while the one Drumbeg Complex sample (Fig. 7f) shows a flat pattern ($[Nb/Yb]_N$ = 0.8) and significant overlap with the Ben Strome field, this sample shows positive La-Ce-Sr-Nd anomalies. The Gorm Chnoc mafic rocks (Fig. 7h) display mild-moderate trace element depletion relative to the Ben Strome Complex, with pronounced negative Nb-Ta-Zr-Hf anomalies ($[Nb/Yb]_N$ = 0.2 – 0.3; $[La/Ta]_N$ = 2.0 – 5.2). Despite showing a significantly larger range in trace element abundances when compared to the Ben Strome Complex, the Geodh' nan Sgadan Complex also displays flat trace element patterns ($[Nb/Yb]_N$ = 0.5 – 1.5), while selected samples show enrichment in Rb and Ba (Fig. 7g).

### *Platinum-group elements and gold*

*Ultramafic rocks*

On chondrite-normalised PGE (+Au) plots, the Ben Strome Complex ultramafic rocks (Fig. 8) exhibit mild to moderately fractioned PGE patterns ($[Pd/Ir]_N$ = 2 – 33), with positively sloping Ir-group PGE (IPGE) with $[Ru/Os]_N$ = 1.4 – 3.9 and near-flat to positively sloping Pd-group PGE (PPGE) where

$[Pd/Rh]_N$ = 0.7 – 5.1. This overall PGE fractionation is replicated by the Achiltibuie ($[Pd/Ir]_N$ = 4.8 – 9.3), Achmelvich ($[Pd/Ir]_N$ = 6.0 – 10.6), Ben Dreavie ($[Pd/Ir]_N$ = 7.2 – 15.6), Drumbeg ($[Pd/Ir]_N$ = 3.5 – 8.4), Loch Eilean na Craoibhe Moire ($[Pd/Ir]_N$ = 1.6 – 12.9), North Scourie Bay ($[Pd/Ir]_N$ = 10.3) and Scouriemore ($[Pd/Ir]_N$ = 1.9 – 25.5) Complexes (Fig. 8). The ultramafic rocks from the Gorm Chnoc and Loch an Daimh Mor Complexes, however, show patterns that are distinctive from this group of complexes. The Gorm Chnoc samples are strongly fractionated ($[Pd/Ir]_N$ = 117 – 124) and relatively depleted in IPGE (Fig. 8h). The Loch an Daimh Mor Complex samples can be subdivided into two groups. The first subgroup (n=3) shows flat to negatively sloping PGE patterns ($[Pd/Ir]_N$ = 0.2 – 1.2), negatively sloping IPGE ($[Ru/Os]_N$ = 0.3 – 0.5) and negatively sloping to flat PPGE ($[Pd/Rh]_N$ = 0.3 – 1.6). The second subgroup (n=3) exhibits positively sloping PGE patterns ($[Pd/Ir]_N$ = 2.2 – 4.2), positively sloping to flat IPGE ($[Ru/Os]_N$ = 1.1 – 9.9) and positively sloping to flat PPGE ($[Pd/Rh]_N$ = 1.6 – 3.5).

*Mafic rocks*

The Ben Strome Complex mafic rocks (Fig. 8) exhibit moderately fractionated PGE patterns ($[Pd/Ir]_N$ = 24 – 46), with this pattern broadly consistent with the Ben Auskaird samples ($[Pd/Ir]_N$ = 18 – 44; Fig. 8c). The Geodh' nan Sgadan mafic rocks (Fig. 8g) also exhibit broadly fractionated patterns ($[Pd/Ir]_N$ = 8 – 24), but, in contrast to Ben Strome, this pattern comprises positively sloping IPGE ($[Ru/Os]_N$ = 10 – 25) and negatively sloping PPGE ($[Pd/Rh]_N$ = 0.3 – 0.7).

## DISCUSSION

The Central Region LGC records a protracted magmatic and metamorphic history that includes at least 3 peaks of amphibolite- to granulite-facies metamorphism. This tectonothermal history, which spans 1 billion years, is associated with polyphase deformation, metasomatism, and partial melting of felsic, intermediate and some mafic lithologies (Johnson et al., 2012; Park et al., 2002). As noted by Johnson et al. (2016), this generates inherent ambiguity when attempting to unpick primary geochemical signatures and interpret the origin and geodynamic significance of ultramafic-mafic

rocks. Moreover, as demonstrated by Guice et al. (2018b), metasomatic effects in the LGC can be both cryptic and extremely localised. These authors show that the LREE – elements typically considered relatively immobile – were enriched in selected samples during interaction with $CO_2$- and $H_2O$-rich fluids, generating apparent negative high field strength element (HFSE) anomalies which, out of context, may have been interpreted as evidence for subduction-related magmatism.

This local variation in deformation, metamorphism and metasomatism is considered throughout the succeeding sections, which aim to unravel the primary geological and geochemical characteristics of the ultramafic-mafic complexes studied. As stated in the Introduction, the paper specifically aims to: (i) examine the validity of the layered intrusion hypothesis ("Ben Strome model") for other ultramafic-mafic complexes in the Central Region LGC; and (ii) if/where this hypothesis fails, assess the possibility that fragments of Archaean mantle may be preserved within this portion of the North Atlantic Craton.

Aim (i) is addressed in the first section of the discussion, with the second and third sections tackling aim (ii). Reference is made throughout to Table 3, which summarises the geochemical features of each ultramafic-mafic complex studied.

### *The Ben Strome Complex: unique occurrence or type locality?*

Seven of the studied complexes – Achiltibuie, Achmelvich, Ben Auskaird, Drumbeg, Loch Eilean na Craoibhe Moire, North Scourie Bay and Scouriemore – display field relationships and geochemical characteristics that are near-identical to those of the Ben Strome Complex (Table 3). Such field characteristics include: a predominance of metapyroxenite in the ultramafic portions; pronounced mm- to m-scale layering in ultramafic lithologies (Fig. 3a-c); relatively discrete layering in the mafic rocks that is defined by the proportions of garnet, pyroxene and plagioclase (Fig. 3d); and consistent parallelism between the layering in the ultramafic-mafic rocks, foliation in the TTG gneiss, and lithological contacts, irrespective of the dominant structural regime (Fig. 2). These common field observations are compounded by the consistent geochemical characteristics shown by this group of

complexes (Table 3; Figs. 5-8), which includes: flat chondrite-normalised REE patterns for ultramafic rocks (Fig. 6); negatively- to positively-sloping, chondrite-normalised REE patterns for mafic rocks (Fig. 6); flat primitive mantle-normalised trace elements for ultramafic rocks (Fig. 7); mildly- to moderately-fractionated PGE patterns for ultramafic rocks (Fig. 8); and moderately fractionated PGE patterns for mafic rocks (Fig. 8). These consistent salient features indicate that this group of complexes likely share a common and broadly contemporaneous origin with the Ben Strome Complex.

Based on field observations, detailed mapping and spinel mineral chemistry, Guice et al. (2018a) suggested that the Ben Strome Complex (and therefore this group of complexes collectively) most likely represents a layered intrusion(s). The field characteristics reported here support this hypothesis, with these other occurrences also exhibiting field features characteristic of layered intrusions (Namur et al. 2015), such as: gradational contacts between ultramafic and mafic units; gradational contacts between metaperidotites and metapyroxenite layers in the ultramafic portions; gradational variation in modal mineral proportions within individual layers; multiple ultramafic and mafic packages occurring within single continuous successions (known as “megacyclic units”; Fig. 2); and truncation of layers on the centimetre- to metre-scale (Fig. 3b-c). This hypothesis is also supported by the geochemical data presented in this paper, with ultramafic and mafic rocks from the 8 complexes (including Ben Strome) collectively displaying: fractionated trends on major element bivariate plots (Fig. 5); and mild- to moderately- fractionated PGE patterns that are typical of layered intrusions (Barnes et al., 1985; Power et al., 2000).

As addressed by Guice et al. (2018a), a layered intrusion interpretation does not, however, solve the crucial age relationship quandary. The field mapping presented in Figure 2 (this study) and by Guice et al. (2018a) highlights the extremely varied and seemingly chaotic map-scale morphologies displayed by this group of complexes. On the one hand, this observation may be used as evidence supporting an interpretation whereby these complexes pre-date the TTG magmas. However,

unambiguous field evidence in the form of cross-cutting relationships are strikingly absent. Moreover, none of the complexes show a spatial association with centimetre- to metre-scale ultramafic-mafic pods in the surrounding TTG gneiss, which are used to infer such age relationships elsewhere in the North Atlantic Craton (Whitehouse and Fedo, 2003). Rather than representing a chaotic distribution caused by fragmentation by TTG magmas, the morphologies displayed by these complexes can instead be attributed to local variation in the predominant structural regime. For example, the Ben Strome and Drumbeg (Fig. 2b) Complexes show Badcallian to Inverian folds that are cross-cut by both Scourie Dykes and Laxfordian shear zones. In contrast, the Loch Eilean na Craoibhe Moire Complex (Fig. 2a), which is located less than 1 km south of the Laxford Shear Zone, show a steeply-dipping, Laxfordian trend that is cross-cut by Scourie Dykes and NE-SW-trending Phanerozoic faults. This strongly suggests that the spatial distribution of ultramafic-mafic rocks reflects the polyphase deformation, rather than primary magmatic fragmentation by TTG magmas.

In the absence of unambiguous cross-cutting relationships, a simple model is proposed, whereby this suite of complexes represent several layered intrusions that were emplaced *into* TTG prior to polyphase deformation and metamorphism (Guice et al., 2018a). It should be noted that because all observed contacts between ultramafic-mafic rocks and the surrounding TTG gneiss are tectonic, such intrusions were not necessarily emplaced into the specific felsic rocks with which they are today juxtaposed. This hypothesis is consistent with the Re-Os isotopic study of Burton et al. (2000) and with recent zircon geochronology conducted by Taylor et al. (2020). In this scenario, it likely that some of the adjacent complexes studied here (i.e., Scouriemore and North Scourie Bay; or Ben Strome and Ben Dreavie) may represent the dismembered fragments of originally continuous layered intrusions (Fig. 9). To answer the question posed in the title of this subsection, the Ben Strome Complex can be considered the type locality for this type of ultramafic-mafic body in the Central Region LGC. This finding represents a significant re-evaluation of the LGC's magmatic evolution, with at least 8 ultramafic-mafic complexes suggested to post-date, rather than pre-date, the TTG magmas, and is outlined in Figure 9.

### *Affiliation of the other ultramafic-mafic bodies*

The remaining 4 complexes – Ben Dreavie, Geodh' nan Sgadan, Gorm Chnoc and Loch an Daimh Mor – exhibit some distinction from the group of Ben Strome-type complexes described above. This section assesses whether such variation can be attributed to a distinctive origin, or whether local variation in metamorphism, metasomatism and/or deformation is instead responsible. We aim to test the hypothesis that the LGC records multiple phases of Archaean ultramafic-mafic magmatism (Guice et al., 2018a; Rollinson and Gravestock, 2012).

*Ben Dreavie: a Ben Strome-type complex*

The Ben Dreavie Complex is comparable to the Ben Strome-type complexes in terms of field relationships, major and minor-element geochemistry (Fig. 5) and PGE geochemistry (Fig 8; Table 3). For example, distinctive layering is prominent in the metapyroxenite-dominated ultramafic rocks, comparable ranges are observed in all major and minor elements, and the PGE patterns are fractionated ($[Pd/Ir]_N$ = 3 – 8). In contrast to the Ben Strome-type complexes, the small number of ultramafic rocks from the complex (n=2) display distinctive chondrite-normalised REE and primitive mantle-normalised trace element patterns, with LREE enrichment ($[La/Ta]_N$ = 6 – 32) and associated HFSE anomalies (Figs. 6-7; Table 3). Despite this, the primitive mantle-normalised Nb/Yb ratios are near-identical ($[Nb/Yb]_N$ = 0.5 – 1.6) to those of the Ben Strome Complex ($[Nb/Yb]_N$ = 0.4 – 3.9), with the Ben Dreavie samples showing almost complete overlap with this field (Fig. 7). Moreover, this trace element pattern, whereby apparent negative HFSE anomalies are associated with LREE enrichment, strongly resembles those described in selected samples from the Ben Strome Complex (Guice et al., 2018b), with localised LREE enrichment by metasomatism associated with $H_2O$ and $CO_2$-rich fluids during amphibolitisation. Corresponding enrichment of Ba and Sr in the Ben Dreavie samples – typically fluid mobile elements – suggests that similar, secondary, processes may have also generated the anomalies in this instance, particularly given the proximal location of the Ben Strome Complex (Fig. 1). While this hypothesis requires assessment by more detailed investigation,

the simplest explanation is that the Ben Dreavie Complex shares a common, layered intrusion, origin with the Ben Strome-type complexes, with the only distinguishing feature – LREE enrichment – likely associated with local metasomatic processes.

*Loch an Daimh Mor: evidence for multiple phases of magmatism in the LGC*

The Loch an Daimh Mor Complex is distinguished from the Ben Strome-type complexes based on several field observations and geochemical characteristics, including (Table 3): the predominance of metaperidotite (Figs. 2 and 3); restriction of metapyroxenite to late, cross-cutting veins, rather than layers (Figs. 2 and 3); occurrence as irregularly-shaped, decimetre-scale pods (Fig. 2); local abundance of Cr-spinel; the map-scale discordance between pod margins and the foliation in the TTG (Fig. 2); the relative $SiO_2$ and NiO enrichment and $Cr_2O_3$, $Fe_2O_3$, $Al_2O_3$ and CaO depletion (Fig. 5); HREE-depleted, LREE-enriched REE patterns (Fig. 6); depletion of the most compatible and most incompatible elements on primitive mantle-normalised trace-element plots (Fig. 7); and the flat to negatively sloping PGE patterns shown by a selection of samples (Fig. 8). It is difficult to envisage a scenario in which all these diverse features can be explained by metamorphism, metasomatism and deformation of an ultramafic-mafic complex that originally resembled Ben Strome. Why, for example, are the ultramafic rocks composed almost exclusively of metaperidotite, when this lithology is extremely rare in the Ben Strome-type complexes? How would a metasomatic process(es) enrich the Loch an Daimh Mor rocks in $SiO_2$, NiO and the IPGE, whilst depleting them in $Cr_2O_3$, $Fe_2O_3$, $Al_2O_3$, CaO and the HREE? Whilst impossible to discount completely without conducting detailed investigations, it appears highly unlikely, based on the evidence presented here, that the characteristics described above can be attributed to a unique suite of metamorphic and metasomatic processes. Instead, we consider it most likely that the Loch an Daimh Mor Complex records an origin distinctive from the Ben Strome-type complexes, supporting the hypothesis that the LGC records multiple petrogenetically distinct suites of Archaean ultramafic-mafic magmatism (Fig. 9). The specific origin is discussed further is a subsequent section.

*Geodh' nan Sgadan and Gorm Chnoc: unknown affiliation*

The Geodh' nan Sgadan Complex is distinguished from the Ben Strome-type complexes based on: extremely prominent and varied layering in the mafic rocks; an abundance of centimetre-scale pods in the surrounding TTG gneiss; rarity and restriction of garnet to rare, centimetre-scale layers; minor depletion in $TiO_2$ and $Fe_2O_3$ on major element bivariate plots (Fig. 5); a relatively broad range of chondrite-normalised REE and primitive mantle-normalised trace element abundances (Figs. 6-7); and flat PPGE patterns (Rh-Pd; Fig. 8). Despite this, these rocks show significant overlap with the Ben Strome Complex on almost all major and minor-element bivariate plots (Fig. 5), and show broad REE and trace-element patterns that are roughly comparable to this field (Figs. 6-7). It is possible that some of the aforementioned distinctions are a consequence of the Geodh' nan Sgadan Complex comprising 100 % mafic rocks, which are relatively susceptible to the high-grade metamorphism and associated partial melting. However, this does not explain the presence of the centimetre-scale pods in the surrounding TTG, which are never observed in association with the Ben Strome-type complexes. We therefore suggest that the Geodh' nan Sgadan Complex could represent a different, perhaps older, protolith that fragmented into the TTG during deformation, but further evidence is required.

The Gorm Chnoc Complex is comparable to the Ben Strome-type complexes in terms of field relationships, major element geochemistry and REE geochemistry, but can be distinguished from this group based on the primitive mantle-normalised trace element patterns (Fig. 7) and the extremely fractionated ($[Pd/IR]_N$ = 117 – 124) chondrite-normalised PGE patterns (Fig. 8; Table 3). On trace element plots, the Gorm Chnoc ultramafic rocks display negative Nb-Ta-Zr-Hf anomalies, but, unlike Ben Dreavie, these samples lack the associated enrichment of LREE and elements typically considered fluid mobile (e.g., Ba), suggesting these anomalies could be primary. This, combined with the distinctive PGE patterns, implies that the Gorm Chnoc Complex is distinct from both the Ben Strome-type and Loch an Daimh Mor complexes. However, the consistency in terms of field relationships, major element geochemistry and REE geochemistry questions this assertion.

Moreover, its location within the Laxford Shear Zone requires caution, with metasomatism highly likely in this region. Ultimately, based on the current data, it is difficult definitively determine whether the Gorm Chnoc Complex represents a distinct magmatic protolith, or whether it is a more intensely metasomatised equivalent of the Ben Strome-type Complexes.

***Loch an Daimh Mor: a fragment of Archaean mantle?***

On the map-scale, the Loch an Daimh Mor Complex occurs as large pods within the TTG gneiss, displaying significant discordance between the gneissose foliation and lithological contacts (Fig. 2c). Although there is no direct evidence of TTG cross-cutting the ultramafic rocks, this map-scale morphology and associated discordance hints that this complex may pre-date the TTG, as previously suggested for all of the ultramafic-mafic complexes in the LGC (Park et al., 2002; Sills, 1981). Given the reported crystallisation ages for the Central Region TTG, which range from 3.1 to 2.8 Ga and are based on U-Pb zircon geochronology (e.g., Kinny et al., 2005; Kinny and Friend, 1997; Love et al., 2010; MacDonald et al., 2015), a precise minimum age is impossible to reconcile for this complex. If the outlined age relationship is correct, these ultramafic rocks must be at least 2.8 Ga (based on the youngest reported crystallisation age for TTG protoliths in the Central Region LGC), but could have a minimum age of 3.05 Ga. This is dependent upon the crystallisation age of the TTG gneiss that are immediately adjacent to the Loch an Daimh Mor Complex, which have not yet been subject to U-Pb zircon geochronology.

Using the criteria developed by Rollinson (2007), we here test the possibility that the Loch an Daimh Mor Complex represent a fragment of Archaean mantle. Further to Figures 6, 7 and 8, which include a comparison to oceanic residue, Figure 10 utilises the Mg/Si versus Al/Si and chondrite-normalised Yb versus Ce/Sm plots. The Loch an Daimh Mor samples are compared to: abyssal peridotites, fore-arc and sub-arc serpentinites, the Oman Ophiolite; orogenic peridotites; and, for a comparison to ultramafic rocks produced by very different mantle-melting processes, komatiites. The other complexes assessed as part of this study are also plotted for reference, with these rocks generally

plotting well outside of the field for abyssal peridotites and overlapping with the komatiites field on the Al/Si versus Mg/Si plot (Fig. 10a). Moreover, on the chondrite-normalised Yb versus Ce/Sm plot, the samples from the other studied complexes largely plot outside of the variety of mantle fields included for reference (Fig. 10b). As outlined in the introduction to this discussion, the complex tectonothermal history experienced by the LGC has likely resulted in (often cryptic) element mobility that can only be constrained by detailed investigations of individual localities (Guice et al., 2018b; Rollinson and Gravestock, 2012). Consequently, these plots should be treated with caution.

For the Loch an Daimh Mor Complex ultramafic rocks, the flat to negatively sloping chondrite-normalised PGE patterns are comparable to those displayed by the mantle portions of ophiolites (Barnes et al., 1985). This similarity is also observed on the Al/Si versus Mg/Si plots, on which 4 of the 5 samples fall within the abyssal peridotites field (Fig. 10a), and on the chondrite-normalised Yb versus Ce/Sm plot, where the samples overlap with the orogenic peridotites field (Fig. 10b). However, this geochemical comparison is contradicted by the chondrite-normalised REE abundances, which are 1-2 orders of magnitude greater than those for residual mantle rocks (Godard et al., 2008, 2000; Paulick et al., 2006; Fig. 6). While it is possible that these REE concentrations reflect mantle metasomatism and re-fertilisation of Archaean mantle, this interpretation requires a huge leap of faith based on the data presented here, particularly given the potentially profound implications for Archaean geodynamic regimes. Ultimately, the Loch an Daimh Mor Complex represents the strongest candidate for Archaean mantle yet discovered in the LGC, but further investigation is required to rigorously test this interpretation.



## CONCLUSIONS

1. A suite of 8 ultramafic-mafic complexes – Achiltibuie, Achmelvich, Ben Auskaird, Ben Dreavie, Drumbeg Loch Eilean na Craoibhe Moire, North Scourie Bay and Scouriemore – share a common origin with the Ben Strome Complex, displaying consistent field relationships and geochemical characteristics. These Ben Strome-type complexes likely represent a suite of layered intrusions that

were emplaced into the TTG prior to polyphase deformation and metamorphism. This finding is a significant re-evaluation of the LGC's magmatic evolution, with the majority of ultramafic-mafic bodies not predating the TTG, as previously assumed.

2. One ultramafic-mafic complex – Loch an Daimh Mor – is considered to unequivocally record an origin distinctive from that of the Ben Strome-type complexes, supporting the hypothesis that the LGC records multiple phases of petrogenetically and temporally distinct Archaean ultramafic-mafic magmatism. This demonstrates that ultramafic-mafic rocks in Archaean cratons, which are sometimes assumed to share a common origin, may record temporal snapshots of specific Archaean processes that can be used to reconstruct processes of cratonisation. The Loch an Daimh Mor Complex represents the strongest candidate for Archaean mantle yet discovered in the LGC, displaying some geochemical characteristics that resemble abyssal and orogenic peridotites.

**ACKNOWLEDGEMENTS AND FUNDING**

G.L.G. would like to thank The Society of Economic Geologists (Graduate Fellowship Award) and The Geological Society (Timothy Jefferson Fund) for generous bursaries that provided funding for the fieldwork upon which this research is based. G.L.G. would also like to thank: Duncan Muir for A-SEM related assistance; Tony Oldroyd for the timely production of high quality thin sections; the Grosvenor Estate for access to the Ben Strome field area; and Alan Hastie and Åke Fagereng, who provided helpful and encouraging comments on the thesis chapter that forms the basis of this paper. The manuscript also benefited from discussions with Kathryn Goodenough and Kate Abernethy. We would like to sincerely thank Tim Johnson and Hugh Rollinson, whose comments on a previous version of the manuscript greatly improved the clarity and quality of this paper. We would also like to thank Tim Johnson (again) and an anonymous reviewer, whose helpful comments helped to further improve this manuscript.

## TABLES AND CAPTIONS

Table 1: Modal mineral proportions for the studied ultramafic rocks. Abbreviations: EM? = element map?; ol = olivine; srp = serpentine; opx = orthopyroxene; cpx = clinopyroxene; amf = amphibole; spn = spinel. *From Guice et al. (2018b). ^excludes vein samples.

| Complex | Sample | Grid ref (NC) | EM? | ol | srp | opx | cpx | amf | spn |
|---|---|---|---|---|---|---|---|---|---|
| Achiltibuie | Lw16_799A | 03048/07951 | Y | 8.8 | 0.0 | 19.0 | 36.9 | 34.4 | 1.0 |
| Achiltibuie | Lw16_799B | 03048/07951 | Y | 2.0 | 8.1 | 50.2 | 7.8 | 30.9 | 1.1 |
| Achmelvich | Lw16-619B | 05749/24184 | Y | 0.0 | 0.0 | 0.0 | 0.0 | 100.0 | 0.0 |
| Achmelvich | Lw16-620A | 05586/24174 | Y | 0.0 | 0.0 | 0.0 | 1.7 | 98.4 | 0.0 |
| Achmelvich | LW17-Am2 | 05688/24284 | Y | 0.0 | 0.0 | 4.3 | 0.0 | 95.0 | 0.8 |
| Ben Dreavie | LW17-BD1 | 26738/38805 | Y | 0.0 | 0.0 | 84.3 | 14.8 | 0.0 | 0.9 |
| Ben Dreavie | LW17-BD2 | 26738/38805 | Y | 2.5 | 2.9 | 51.1 | 29.1 | 13.3 | 1.1 |
| Drumbeg | LW17-Db3b | 11067/33060 | Y | 0.0 | 32.4 | 30.8 | 9.0 | 26.5 | 1.4 |
| Drumbeg | LW17-Db8 | 11255/33061 | Y | 2.0 | 18.6 | 7.9 | 0.0 | 70.4 | 1.2 |
| Drumbeg | LW17-44 | 11472/33323 | Y | 0.0 | 5.2 | 52.1 | 13.7 | 28.7 | 0.4 |
| Drumbeg | LW17-45A | 11455/33353 | | 1.5 | 0.5 | 52.0 | 5.0 | 39.0 | 2.0 |
| Gorm Chnoc | LW17-GC2 | 21912/44749 | Y | 0.4 | 7.0 | 31.6 | 6.7 | 54.0 | 0.2 |
| Gorm Chnoc | LW17-GC3 | 21912/44749 | | 1.5 | 15.0 | 8.0 | 18.0 | 55.0 | 2.5 |
| Gorm Chnoc | LW17-GC5 | 21954/44751 | Y | 4.7 | 28.1 | 2.8 | 0.0 | 64.4 | 0.0 |
| Loch Eilean na Craoibhe Moire | Lw16_627B | 21188/43446 | | 0.0 | 0.0 | 39.8 | 10.0 | 50.0 | 0.2 |
| Loch Eilean na Craoibhe Moire | Lw16_629B | 21127/43493 | Y | 0.0 | 0.0 | 42.4 | 2.9 | 50.9 | 3.9 |
| Loch Eilean na Craoibhe Moire | LW17-E1 | 21448/43096 | Y | 0.0 | 0.0 | 16.1 | 33.4 | 49.9 | 0.6 |
| Loch Eilean na Craoibhe Moire | LW17-E2A | 21448/43096 | Y | 0.0 | 9.3 | 38.0 | 6.4 | 46.4 | 0.0 |
| Loch Eilean na Craoibhe Moire | LW17-E2B | 21448/43096 | | 4.5 | 1.0 | 25.0 | 45.0 | 23.0 | 1.5 |
| Loch Eilean na Craoibhe Moire | LW17-E2C | 21448/43096 | | 15.5 | 26.0 | 40.0 | 12.0 | 4.0 | 2.5 |
| Loch Eilean na Craoibhe Moire | LW17-E3 | 21448/43096 | Y | 0.0 | 19.1 | 42.8 | 6.9 | 31.2 | 0.0 |
| Loch Eilean na Craoibhe Moire | LW17-E5 | 21448/43096 | Y | 4.0 | 10.2 | 48.0 | 8.3 | 28.3 | 1.2 |
| Loch an Daimh Mor | UBCr_P1 | | Y | 0.0 | 40.7 | 56.5 | 1.2 | 0.0 | 1.6 |
| Loch an Daimh Mor | UBCr_P3 | | Y | 0.0 | 37.5 | 42.2 | 6.7 | 12.5 | 1.2 |
| Loch an Daimh Mor | X11A | | Y | 0.0 | 54.5 | 5.9 | 0.0 | 39.6 | 0.0 |
| Loch an Daimh Mor | X11B | | | 0.0 | 100.0 | 0.0 | 0.0 | 0.0 | 0.0 |
| Loch an Daihm Mor - vein | UBZr_1a | | | 0.0 | 25.0 | 60.0 | 5.0 | 10.0 | 0.0 |
| Loch an Daihm Mor - vein | LEW014A | 15621/41834 | Y | 0.0 | 0.0 | 97.1 | 0.2 | 2.7 | 0.0 |
| North Scourie Bay | NSB_UMa | | | 0.0 | 0.0 | 75.0 | 0.0 | 23.0 | 2.0 |
| North Scourie Bay | NSB_UMb | | | 3.5 | 0.0 | 31.0 | 31.0 | 33.0 | 1.5 |
| Scouriemore | T2190 | | Y | 0.0 | 4.0 | 7.4 | 48.1 | 37.6 | 2.9 |
| Scouriemore | T2160L | | Y | 0.0 | 20.0 | 37.5 | 19.0 | 21.1 | 2.4 |
| Scouriemore | T2160U | | y | 0.0 | 18.9 | 45.7 | 26.6 | 7.1 | 1.7 |
| Scouriemore | T2110 | | Y | 0.0 | 0.0 | 20.4 | 22.6 | 54.7 | 2.3 |
| Scouriemore | X3 | | Y | 0.0 | 0.0 | 0.0 | 0.2 | 99.8 | 0.0 |
| Scouriemore | Lw16_643B | 14230/44184 | Y | 19.0 | 0.0 | 40.5 | 18.4 | 21.0 | 1.0 |
| Scouriemore | Lw16_657 | 14209/44227 | Y | 0.0 | 0.0 | 28.8 | 23.8 | 44.8 | 2.6 |
| **Average** | | | | **ol** | **srp** | **opx** | **cpx** | **amf** | **spn** |
| *Ben Strome (n=33)** | | | | *1* | *30* | *27* | *17* | *24* | *1* |
| Achiltibuie (n=2) | | | | 5 | 4 | 35 | 22 | 33 | 1 |
| Achmelvich (n=2) | | | | 0 | 0 | 0 | 1 | 99 | 0 |
| Ben Dreavie (n=2) | | | | 1 | 1 | 68 | 22 | 7 | 1 |
| Drumbeg (n=4) | | | | 1 | 14 | 36 | 7 | 41 | 1 |
| Gorm Chnoc (n=3) | | | | 2 | 17 | 14 | 8 | 58 | 1 |
| Loch Eilean na Craoibhe Moire (n=8) | | | | 3 | 8 | 37 | 16 | 35 | 1 |
| Loch an Daimh Mor (n=4)^ | | | | 0 | 58 | 26 | 2 | 13 | 1 |
| North Scourie Bay (n=2) | | | | 2 | 0 | 53 | 16 | 28 | 2 |
| Scourimore (n=7) | | | | 3 | 6 | 26 | 23 | 41 | 2 |
| **Range** | | | | **ol** | **srp** | **opx** | **cpx** | **amf** | **spn** |
| *Ben Strome* | | | | *< 5* | *< 100* | *< 91* | *< 45* | *< 78* | *< 5* |
| Achiltibuie | | | | 2 – 9 | < 8 | 19 - 50 | 8 - 37 | 31 - 35 | 1 |
| Achmelvich | | | | 0 | 0 | < 4.3 | < 1.7 | > 95 | < 1 |
| Ben Dreavie | | | | < 2.5 | < 3 | 51 - 84 | 15 - 30 | < 13 | 1 |
| Drumbeg | | | | < 2 | < 32 | 8 - 52 | < 14 | 27 - 70 | < 2 |
| Gorm Chnoc | | | | < 5 | 7 - 28 | 3 - 32 | < 18 | 54 - 64 | < 2.5 |
| Loch Eilean na Craoibhe Moire | | | | < 16 | 26 | 16 - 48 | 3 - 45 | 4 - 51 | < 4 |

| | | | | | | |
|---|---|---|---|---|---|---|
| Loch an Daimh Mor | 0 | > 38 | < 57 | < 7 | < 40 | < 2 |
| North Scourie Bay | < 3.5 | 0 | 31 - 75 | < 31 | 23 - 33 | 1.5 - 2 |
| Scourimore | < 19 | < 20 | < 46 | < 48 | > 7 | < 3 |

Table 2: Modal mineral proportions for the studied mafic rocks. Abbreviations: EM? = element map?; opx = orthopyroxene; cpx = clinopyroxene; amf = amphibole; fel = feldspar; gnt = garnet; qtz = quartz; ox = oxide minerals.

| Complex | Sample | Grid ref (NC) | EM? | opx | cpx | amf | fel | gnt | qtz | ox |
|---|---|---|---|---|---|---|---|---|---|---|
| Ben Auskaird | LEW004 | 20926/40272 | | 0.0 | 0.0 | 84.0 | 13.0 | 0.0 | 3.0 | 0.0 |
| Ben Strome | LEW010 | 25375/35591 | | 2.0 | 8.0 | 71.0 | 2.0 | 12.0 | 0.0 | 5.0 |
| Ben Strome | LEW011 | 25716/36120 | | 16.0 | 16.0 | 12.0 | 13.0 | 35.0 | 0.0 | 8.0 |
| Ben Strome | LEW012 | 25553/36005 | | 30.0 | 60.0 | 10.0 | 0.0 | 0.0 | 0.0 | 0.0 |
| Ben Strome | Lw16_510b | 24879/35626 | | 8.0 | 22.0 | 11.0 | 27.0 | 32.0 | 0.0 | 0.0 |
| Ben Strome | Lw16_Z2a-1 | 26067/35391 | | 2.0 | 7.0 | 46.0 | 24.5 | 18.0 | 0.5 | 2.0 |
| Ben Strome | Lw16_Z2a-2 | 26067/35391 | | 0.0 | 0.0 | 65.0 | 35.0 | 0.0 | 0.0 | 0.0 |
| Ben Strome | Lw16_Z2b | 26067/35391 | | 5.0 | 30.0 | 65.0 | 0.0 | 0.0 | 0.0 | 0.0 |
| Ben Strome | Lw16_Z13b | 26073/35578 | Y | 0.0 | 2.7 | 51.9 | 45.0 | 0.0 | 0.4 | 0.0 |
| Ben Strome | Lw16_Z13c | 26073/35578 | Y | 0.0 | 35.8 | 39.9 | 15.4 | 7.9 | 1.0 | 0.0 |
| Ben Strome | Lw16_Z14a | 26073/35585 | | 9.0 | 48.0 | 23.0 | 8.0 | 12.0 | 0.0 | 0.0 |
| Ben Strome | Lw16_Z14b | 26073/35585 | | 0.0 | 4.8 | 75.0 | 20.0 | 0.0 | 0.2 | 0.0 |
| Ben Strome | Lw16_Z15 | 26077/35593 | | 0.0 | 49.0 | 20.0 | 18.0 | 11.0 | 0.0 | 2.0 |
| Geodh' nan Sgadan | LW17-BcT3 | 14632/41779 | Y | 11.2 | 0.0 | 82.3 | 6.5 | 0.0 | 0.0 | 0.0 |
| Geodh' nan Sgadan | LW17-BcT4 | 14631/41780 | | 5.0 | 6.0 | 44.0 | 45.0 | 0.0 | 0.0 | 0.0 |
| Geodh' nan Sgadan | LW17-BcT6 | 14628/41784 | Y | 0.0 | 27.9 | 71.5 | 0.0 | 0.0 | 0.6 | 0.0 |
| Geodh' nan Sgadan | LW17-BcT8 | 14627/41801 | Y | 0.0 | 35.4 | 0.0 | 64.1 | 0.0 | 0.0 | 0.5 |
| Geodh' nan Sgadan | LW17-BcT12A | 14625/41836 | | 0.0 | 0.0 | 20.0 | 66.0 | 14.0 | 0.0 | 0.0 |
| Gorm Chnoc | LW17-GC1 | 22139/44569 | | 0.0 | 0.0 | 85.0 | 15.0 | 0.0 | 0.0 | 0.0 |
| Gorm Chnoc | LW17-GC4 | 22156/44613 | | 0.0 | 0.0 | 70.0 | 30.0 | 0.0 | 0.0 | 0.0 |
| **Average** | | | | **opx** | **cpx** | **amf** | **fel** | **gnt** | **qtz** | **ox** |
| *Ben Strome (n=12)* | | | | *6* | *24* | *41* | *17* | *11* | *0* | *1* |
| Ben Auskaird (n=1) | | | | 0 | 0 | 84 | 13 | 0 | 3 | 0 |
| Gorm Chnoc (n=2) | | | | 0 | 0 | 78 | 23 | 0 | 0 | 0 |
| Geodh' nan Sgadan (n=5) | | | | 3 | 14 | 44 | 36 | 3 | 0 | 0 |
| **Range** | | | | **opx** | **cpx** | **amf** | **fel** | **gnt** | **qtz** | **ox** |
| *Ben Strome (n=12)* | | | | < 30 | < 60 | 10 - 75 | < 45 | < 35 | < 1 | < 8 |
| Ben Auskaird (n=1) | | | | 0 | 0 | 84 | 13 | 0 | 3 | 0 |
| Gorm Chnoc (n=2) | | | | 0 | 0 | 70 - 85 | 15 - 30 | 0 | 0 | 0 |
| Geodh' nan Sgadan (n=5) | | | | < 11 | < 35 | < 82 | < 66 | < 14 | < 1 | < 1 |

Table 3: Major, minor, trace and platinum-group element characteristics of the 12 ultramafic-mafic complexes, alongside a comparison between Ben Strome and each complex studied here Abbreviations: LDM = Loch an Daimh Mor; LEC = Loch Eilean na Craoibhe Moire; NSB = North Scourie Bay; GnS = Geodh' nan Sgadan; chonN = chondrite normalised; pmN = primitive mantle normalised; PGE = platinum-group elements. *major, minor and trace elements are from Guice et al. (2018b). PGE are from this study. ^ trace elements are those considered by Guice et al. (2018b) to most closely resemble primary magmatic compositions. Other symbols: tick = comparable to the Ben Strome Complex; cross = distinct from the Ben Strome Complex; backwards slash = relatively minor, but notable distinction. Underlined cross = feature can likely be explained by secondary processes.

| | | Major and minor elements (Fig. 5) | | | | | | | Trace elements (Figs. 6-7) | | | | PGE (Fig. 8) | |
|---|---|---|---|---|---|---|---|---|---|---|---|---|---|---|
| Locality | n= | MgO | $SiO_2$ | $TiO_2$ | $Al_2O_3$ | CaO | $Cr_2O_3$ | NiO | La/Lu | La/Sm | Nb/Yb | La/Ta | Pd/Ir | Total PGE |
| Unit | | wt. % | wt. % | wt. % | wt. % | wt. % | wt. % | wt. % | chonN | chonN | pmN | pmN | chonN | ppb |
| *Ultramafic rocks* | | | | | | | | | | | | | | |
| Ben Strome*^ | 35 | 18 - 48 | 36 - 48 | 0.1 – 0.7 | 2 - 13 | 1 - 12 | 0.1 - 0.5 | 0.1 - 1 | 0.5 - 2 | 0.6 - 2.2 | 0.4 - 3.9 | 0.3 - 2.0 | 2 - 33 | 5 – 34 |
| Achmelvich | 4 | 17 - 28 | 45 - 50 | 0.3 – 0.4 | 6 – 8 | 7 - 10 | 0.3 - 0.5 | 0.1 - 0.8 | 0.4 - 0.6 | 0.3 - 0.5 | 0.4 - 2.5 | 0.6 - 0.8 | 6 - 11 | 9 – 11 |
| Achiltibuie | 3 | 27 - 31 | 45 - 57 | 0.2 – 0.3 | 4 – 6 | 6 - 8 | 0.4 | 0.1 - 0.3 | 0.7 - 2.3 | 0.6 - 1.9 | 0.8 - 2.6 | 0.2 - 0.9 | 5 - 9 | 15 - 24 |
| Ben Dreavie | 2 | 27 - 29 | 47 - 49 | 0.2 – 0.3 | 5 | 3 - 6 | 0.4 | 0.1 - 0.2 | 15 - 20 | 6.1 - 9.7 | 0.5 - 1.6 | 5.8 - 31.5 | 3 - 8 | 33 – 39 |
| Drumbeg | 9 | 21 - 32 | 43 - 47 | 0.2 – 0.6 | 4 – 11 | 5 - 9 | 0.1 - 0.4 | 0.1 - 0.2 | 0.6 - 1.9 | 0.5 - 1.3 | 0.6 - 1.2 | 0.6 - 1.7 | 7 - 16 | 14 – 75 |
| Gorm Chnoc | 3 | 25 - 28 | 40 - 46 | 0.2 – 0.3 | 7 - 10 | 5 - 7 | < 0.4 | 0.1 | 1.8 - 2.1 | 0.6 - 2.1 | 0.5 - 0.6 | 2.8 - 3.2 | 117 - 124 | 18 – 24 |
| LDM | 5 | 35 - 42 | 46 - 51 | < 0.2 | 2 – 4 | < 1.5 | 0.1 - 0.4 | 0.3 - 0.4 | 0.2 - 8.4 | 1.5 - 3.2 | 0.5 - 2.2 | 0.2 - 9.0 | 0.2 - 4 | 3 – 30 |
| LEC | 9 | 26 - 40 | 40 - 49 | 0.1 – 0.4 | 3 – 8 | 1 - 8 | 0.3 - 0.7 | 0.1 - 0.6 | 1.0 - 2.9 | 0.9 - 2.9 | 0.4 - 2.9 | 0.8 - 2.0 | 2 - 13 | 11 – 45 |
| NSB | 1 | 21 | 48 | 0.4 | 7 | 10 | 0.3 | 0.1 | 2.7 | 1.5 | 1.2 | 1.7 | 10 | 22 |
| Scouriemore | 9 | 19 - 31 | 43 - 48 | 0.2 – 0.5 | 5 – 9 | 6 - 14 | 0.3 - 0.5 | 0.1 - 0.2 | 0.8 - 5.0 | 0.7 - 2.2 | 0.6 - 2.2 | 0.7 - 1.7 | 2 - 25 | 13 - 34 |
| Mafic rocks | | | | | | | | | | | | | | |
| Ben Strome | 17 | 5 - 21 | 39 - 49 | 0.3 – 16 | 8 – 17 | 9 - 17 | < 0.2 | < 0.1 | 0.3 - 8 | 0.2 - 3.1 | 0.3 - 1.9 | < 8.8 | 24 - 46 | 1 - 6 |
| Ben Auskaird | 2 | 3 - 4 | 48 - 60 | 3 | 13 | 7 - 8 | < 0.1 | < 0.1 | 2.0 - 3.1 | 1.3 - 2.5 | 2.2 | 0.8 - 1.5 | 18 - 44 | 3 - 18 |
| Drumbeg | 1 | 10 | 49 | 0.9 | 14 | 11 | < 0.1 | < 0.1 | 7 | 1.5 | 0.8 | 8.2 | n/a | n/a |
| GnS | 5 | 5 - 14 | 45 - 54 | 0.2 – 1.6 | 14 – 20 | 9 - 13 | < 0.3 | < 0.1 | 2.0 - 4.7 | 1.7 - 2.8 | 0.5 - 1.5 | 1.6 - 8 | 8 - 24 | 11 – 12 |
| Gorm Chnoc | 2 | 12 - 14 | 48 - 49 | 0.2 | 14 – 15 | 14 | < 0.2 | < 0.1 | 0.6 - 0.9 | 0.6 - 0.8 | 0.2 - 0.3 | 2.0 - 5.2 | n/a | n/a |

**FIGURE CAPTIONS**

Figure 1: Simplified geological map of the LGC detailing the locations of the ultramafic-mafic complexes investigated as part of this study (redrawn after: Johnson et al., 2012; Kinny et al., 2005; Wheeler et al., 2010). Abbreviations: Ac=Achiltibuie; Am=Achmelvich; BA=Ben Auskaird; BD=Ben Dreavie; BS=Ben Strome; Db=Drumbeg; GC=Gorm Chnoc; GnS=Geodh' nan Sgadan; LDM=Loch an Daimh Mor; LE=Loch Eilean na Craoibhe Moire; NSB=North Scourie Bay; Sm=Scouriemore.

Figure 2: Simplified geological maps of the Loch Eilean na Craoibhe Moire, Drumbeg, Loch an Daimh Mor and Gnoc Gorm Complexes. The location of each complex is detailed in Figure 1.

Figure 3: Field photographs detailing the representative rock types that comprise the ultramafic-mafic complexes studied.

Figure 4: Photomicrographs (XPL) detailing the petrographic characteristics of the studied rocks. White scale bar = 1 mm.

Figure 5: Bivariate plots detailing the anhydrous major and minor-element compositions of the ultramafic-mafic rocks analysed from the 12 studied complexes. *Ben Strome data includes 35 ultramafic samples published in Guice et al. (2018b).

Figure 6: Chondrite-normalised (McDonough and Sun, 1995) REE plots for the analysed ultramafic-mafic rocks from the 12 studied complexes.

Figure 7: Primitive mantle-normalised (McDonough and Sun, 1995) trace element plots for the analysed ultramafic-mafic rocks from the 12 studied complexes.

Figure 8: Chondrite-normalised (Lodders, 2003) PGE (+Au) plots for the analysed ultramafic-mafic rocks from the 12 studied complexes. Abbreviations: UM = ultramafic; M = mafic.

Figure 9: Schematic diagram detailing the proposed evolution of the LGC.

Figure 10: (a) Mg/Si versus Al/Si (wt. %) plot for the ultramafic rocks analysed as part of this study. (b) Chondrite-normalised [Ce/Yb] versus [Yb] plot for the ultramafic rocks analysed as part of this study. Fields are after: Rollinson (2007). Abbreviations: PM = primitive mantle. LEC = Loch Eilean na Craoibhe Moire LDM = Loch an Daimh Mor; NSB = North Scourie Bay. * = includes ultramafic samples published by Guice et al. (2018b).

## REFERENCES

Andersen, T., Whitehouse, M.J., Burke, E.A.J., 1997. Fluid inclusions in Scourian granulites from the Lewisian complex of NW Scotland: evidence for CO2-rich fluid in Late Archaean high-grade metamorphism. Lithos 40, 93–104.

Arndt, N.T., 2013. Formation and Evolution of the Continental Crust. Geochemical Perspect. 2, 405–533. https://doi.org/10.7185/geochempersp.2.3

Barnes, S.J., Naldrett, A.J., Gorton, M.P., 1985. The origin of the fractionation of platinum-group elements in terrestrial magmas. Chem. Geol. 53, 303–323. https://doi.org/10.1016/0009-2541(85)90076-2

Barnicoat, A.C., 1983. Metamorphism of the Scourian Complex, NW Scotland. J. Metamorph. Geol. 1, 163–182.

Barnicoat, A.C., O'Hara, M.J., 1978. High-temperature pyroxenes from an ironstone at Scourie, Sutherland. Mineral. Mag. 43, 371–375.

Barooah, B.C., Bowes, D.R., 2009. Multi-episodic modification of high-grade terrane near Scourie and its significance in elucidating the history of the Lewisian Complex. Scottish J. Geol. 45, 19–41. https://doi.org/10.1144/0036-9276/01-384

Beach, A., 1974. Amphibolitization of Scourian granulites. Scottish J. Geol. 10, 35–43.

Beach, A., 1973. The mineralogy of high temperature shear zones at Scourie, N.W. Scotland. J. Petrol. 14, 231–248.

Beach, A., Coward, M.P., Graham, R.H., 1974. An interpretation of the structural evolution of the Laxford Front, north-west Scotland. Scottish J. Geol. 9, 297–308.

Bédard, J.H., 2018. Stagnant lids and mantle overturns : Implications for Archaean tectonics , magmagenesis , crustal growth , mantle evolution , and the start of plate tectonics. Geosci.

Front. 9, 19–49. https://doi.org/10.1016/j.gsf.2017.01.005

Bédard, J.H., Harris, L.B., Thurston, P.C., 2013. The hunting of the snArc. Precambrian Res. 229, 20–48. https://doi.org/10.1016/j.precamres.2012.04.001

Bowen, N.L., 1956. The evolution of igneous rocks. Dover Publications, New York.

Bowes, D.R., Park, R.G., Wright, A.E., 1964. Layered intrusive rocks in the Lewisian of the North-West Highlands of Scotland. Q. J. Geol. Soc. 120, 153. https://doi.org/10.1144/gsjgs.120.1.0153

Brown, M., Johnson, T.E., 2018. Secular change in metamorphism and the onset of global plate tectonics. Am. Mineral. 103, 181–196. https://doi.org/10.2138/am-2018-6166

Burton, K.W., Capmas, F., Birck, J.L., Allegre, C.J., Cohen, A.S., 2000. Resolving crystallisation ages of Archean mafic-ultramafic rocks using the Re-Os isotope system. Earth Planet. Sci. Lett. 179, 453–467.

Cartwright, I., Fitches, W.R., O'Hara, M.J., Barnicoat, A.C., O'Hara, S., 1985. Archaean supracrustal rocks from the Lewisian near Stoer, Sutherland. Scottish J. … 21, 187–196. https://doi.org/10.1144/sjg21020187

Cawood, P.A., Hawkesworth, C.J., Pisarevsky, S.A., Dhuime, B., Capitanio, F.A., Nebel, O., 2018. Geological archive of the onset of plate tectonics. Phil. Trans. R. Soc. Lond. 376.

Condie, K.C., 2018. A planet in transition: The onset of plate tectonics on Earth between 3 and 2 Ga? Geosci. Front. 9, 51–60. https://doi.org/10.1016/j.gsf.2016.09.001

Corfu, F., 1998. U-Pb zircon systematics at Gruinard Bay, northwest Scotland : implications for the early orogenic evolution of the Lewisian complex. Contrib. to Mineral. Petrol. 133, 329–345.

Corfu, F., Heaman, L.M., Rogers, G., 1994. Polymetamorphic evolution of the Lewisian complex, NW Scotland, as recorded by U-Pb isotopic compositions of zircon, titanite and rutile. Contrib. to Mineral. Petrol. 117, 215–228.

Crowley, Q.G., Key, R., Noble, S.R., 2015. High-precision U–Pb dating of complex zircon from the Lewisian Gneiss Complex of Scotland using an incremental CA-ID-TIMS approach. Gondwana Res. 27, 1381–1391. https://doi.org/10.1016/j.gr.2014.04.001

Davies, J.H.F.L., Heaman, L.M., 2014. New U-Pb baddeleyite and zircon ages for the Scourie dyke swarm: A long-lived large igneous province with implications for the Paleoproterozoic evolution of NW Scotland. Precambrian Res. 249, 180–198. https://doi.org/10.1016/j.precamres.2014.05.007

Dhuime, B., Wuestefeld, A., Hawkesworth, C.J., 2015. Emergence of modern continental crust about 3 billion years ago. Nat. Geosci. 8, 552–555. https://doi.org/10.1038/NGEO2466

Evans, C.R., Lambert, R.S.J., 1974. The Lewisian of Lochinver, Sutherland; the type area for the Inverian metamorphism. J. Geol. Soc. London. 130, 125–150. https://doi.org/10.1144/gsjgs.130.2.0125

Faithfull, J.W., Dempster, T.J., MacDonald, J.M., Reilly, M., 2018. Metasomatism and the crystallization of zircon megacrysts in Archaean peridotites from the Lewisian complex, NW Scotland. Contrib. to Mineral. Petrol. 173, 99. https://doi.org/10.1007/s00410-018-1527-5

Feisel, Y., White, R.W., Palin, R.M., Johnson, T.E., 2018. New constraints on granulite facies metamorphism and melt production in the Lewisian Complex, northwest Scotland. J. Metamorph. Geol. 1–21. https://doi.org/10.1111/jmg.12311

Friend, C.R.L., Kinny, P.D., 2001. A reappraisal of the Lewisian Gneiss Complex: geochronological evidence for its tectonic assembly from disparate terranes in the Proterozoic. Contrib. to Mineral. Petrol. 142, 198–218. https://doi.org/10.1007/s004100100283

Furnes, H., Robins, B., De Wit, M.J., 2012. Geochemistry and petrology of lavas in the upper onverwacht suite, Barberton Mountain Land, South Africa. South African J. Geol. 115, 171–210. https://doi.org/10.2113/gssajg.115.2.171

Godard, M., Jousselin, D., Bodinier, J., 2000. Relationships between geochemistry and structure beneath a palaeo-spreading centre: a study of the mantle section in the Oman ophiolite. Earth Planet. Sci. Lett. 180, 133–148.

Godard, M., Lagabrielle, Y., Alard, O., Harvey, J., 2008. Geochemistry of the highly depleted peridotites drilled at ODP Sites 1272 and 1274 (Fifteen-Twenty Fracture Zone, Mid-Atlantic Ridge): Implications for mantle dynamics beneath a slow spreading ridge. Earth Planet. Sci. Lett. 267, 410–425. https://doi.org/10.1016/j.epsl.2007.11.058

Goodenough, K.M., Crowley, Q.G., Krabbendam, M., Parry, S.F., 2013. New u-pb age constraints for the Laxford Shear Zone, NW Scotland: Evidence fortectono-magmatic processes associated with the formation of a paleoproterozoic supercontinent. Precambrian Res. 232, 1–19. https://doi.org/10.1016/j.precamres.2013.05.006

Goodenough, K.M., Park, R.G., Krabbendam, M., Myers, J.S., Wheeler, J., Loughlin, S.C., Crowley, Q.G., Friend, C.R.L., Beach, A., Kinny, P.D., Graham, R.H., 2010. The Laxford Shear Zone: an end-Archaean terrane boundary? Geol. Soc. London, Spec. Publ. 335, 103–120. https://doi.org/10.1144/SP335.6

Guice, G.L., 2019. Origin and geodynamic significance of ultramafic-mafic complexes in the North Atlantic and Kaapvaal Cratons. Cardiff University.

Guice, G.L., McDonald, I., Hughes, H.S.R., Anhaeusser, C.R., 2019. An evaluation of element mobility in the Modderfontein ultramafic complex, Johannesburg: Origin as an Archaean ophiolite fragment or greenstone belt remnant? Lithos 332–333, 99–119. https://doi.org/10.1016/j.lithos.2019.02.013

Guice, G.L., McDonald, I., Hughes, H.S.R., MacDonald, J.M., Blenkinsop, T.G., Goodenough, K.M., Faithfull, J.W., Gooday, R.J., 2018a. Re-evaluating ambiguous age relationships in Archean cratons: Implications for the origin of ultramafic-mafic complexes in the Lewisian Gneiss

Complex. Precambrian Res. 311, 136–156. https://doi.org/10.1016/j.precamres.2018.04.020

Guice, G.L., McDonald, I., Hughes, H.S.R., Schlatter, D.M., Goodenough, K.M., Macdonald, J.M., Faithfull, J.W., 2018b. Assessing the Validity of Negative High Field Strength-Element Anomalies as a Proxy for Archaean Subduction: Evidence from the Ben Strome Complex, NW Scotland. Geosciences 8, 338. https://doi.org/10.3390/geosciences8090338

Halla, J., 2018. Highlights on Geochemical Changes in Archaean Granitoids and Their Implications for Early Earth Geodynamics. Geosciences 8, 353. https://doi.org/10.3390/geosciences8090353

Heaman, L.M., Tarney, J., 1989. U–Pb Baddeleyite ages for the Scourie Dyke Swarm, Scotland – evidence for 2 distinct intrusion events. Nature 340, 705–708.

Huber, H., Koeberl, C., McDonald, I., Reimold, W.U., 2001. Geochemistry and petrology of Witwatersrand and dwyka diamictites from south Africa: Search for an extraterrestrial component. Geochim. Cosmochim. Acta 65, 2007–2016. https://doi.org/10.1016/S0016-7037(01)00569-5

Johnson, T.E., Brown, M., Gardiner, N.J., Kirkland, C.L., Smithies, R.H., 2017. Earth's first stable continents did not form by subduction. Nature. https://doi.org/10.1038/nature21383

Johnson, T.E., Brown, M., Goodenough, K.M., Clark, C., Kinny, P.D., White, R.W., 2016. Subduction or sagduction ? Ambiguity in constraining the origin of ultramafic – mafic bodies in the Archean crust of NW Scotland. Precambrian Res. 283, 89–105. https://doi.org/10.1016/j.precamres.2016.07.013

Johnson, T.E., Fischer, S., White, R.W., 2013. Field and petrographic evidence for partial melting of TTG gneisses from the central region of the mainland Lewisian complex, NW Scotland. J. Geol. Soc. London. 170, 319–326. https://doi.org/10.1144/jgs2012-096

Johnson, T.E., Fischer, S., White, R.W., Brown, M., Rollinson, H.R., 2012. Archaean intracrustal differentiation from partial melting of metagabbro-field and geochemical evidence from the

central region of the Lewisian complex, NW Scotland. J. Petrol. 53, 2115–2138. https://doi.org/10.1093/petrology/egs046

Johnson, T.E., Kirkland, C.L., Gardiner, N.J., Brown, M., Smithies, R.H., Santosh, M., 2019. Secular change in TTG compositions: Implications for the evolution of Archaean geodynamics. Earth Planet. Sci. Lett. 505, 65–75. https://doi.org/10.1016/j.epsl.2018.10.022

Kamber, B.S., 2015. The evolving nature of terrestrial crust from the Hadean, through the Archaean, into the Proterozoic. Precambrian Res. 258, 48–82. https://doi.org/10.1016/j.precamres.2014.12.007

Kinny, P., Friend, C., Love, G., 2005. Proposal for a terrane-based nomenclature for the Lewisian Gneiss Complex of NW Scotland. J. Geol. Soc. London. 162, 175–186. https://doi.org/10.1144/0016-764903-149

Kinny, P.D., Friend, C.R.L., 1997. U-Pb isotopic evidence for the accretion of different crustal blocks to form the Lewisian Complex of northwest Scotland. Contrib. to Mineral. Petrol. 129, 326–340. https://doi.org/10.1007/s004100050340

Lodders, K., 2003. Solar System Abundances and Condensation Temperatures of the Elements. Astrophys. J. 591, 1220–1247. https://doi.org/10.1086/375492

Love, G.J., Friend, C.R.L., Kinny, P.D., 2010. Palaeoproterozoic terrane assembly in the Lewisian Gneiss Complex on the Scottish mainland, south of Gruinard Bay: SHRIMP U-Pb zircon evidence. Precambrian Res. 183, 89–111. https://doi.org/10.1016/j.precamres.2010.07.014

Love, G.J., Kinny, P.D., Friend, C.R.L., 2004. Timing of magmatism and metamorphism in the Gruinard Bay area of the Lewisian Gneiss Complex: Comparisons with the Assynt Terrane and implications for terrane accretion. Contrib. to Mineral. Petrol. 146, 620–636. https://doi.org/10.1007/s00410-003-0519-1

MacDonald, J.M., Goodenough, K.M., Wheeler, J., Crowley, Q., Harley, S.L., Mariani, E., Tatham, D.,

2015. Temperature-time evolution of the Assynt Terrane of the Lewisian Gneiss Complex of Northwest Scotland from zircon U-Pb dating and Ti thermometry. Precambrian Res. 260, 55–75. https://doi.org/10.1016/j.precamres.2015.01.009

McDonald, I., Viljoen, K.S., 2006. Platinum-group element geochemistry of mantle eclogites: a reconnaissance study of xenoliths from the Orapa kimberlite, Botswana. Appl. Earth Sci. 115, 81–93. https://doi.org/10.1179/174327506X138904

McDonough, W.F., Sun, S. s., 1995. The composition of the Earth. Chem. Geol. 120, 223–253. https://doi.org/10.1016/0009-2541(94)00140-4

Moyen, J., Laurent, O., 2018. Archaean tectonic systems : A view from igneous rocks. Lithos 302–303, 99–125. https://doi.org/10.1016/j.lithos.2017.11.038

Park, R.G., 2005. The Lewisian terrane model: a review. Scottish J. Geol. 41, 105–118. https://doi.org/10.1144/sjg41020105

Park, R.G., Stewart, A.D., Wright, A.E., 2002. The Hebridean Terrane, in: The Geology of Scotland.

Park, R.G., Tarney, J., 1987. The Lewisian complex: a typical Precambrian high-grade terrain? Geol. Soc. London, Spec. Publ. 27, 13–25. https://doi.org/10.1144/gsl.sp.1987.027.01.03

Paulick, H., Bach, W., Godard, M., Hoog, J.C.M. De, Suhr, G., Harvey, J., 2006. Geochemistry of abyssal peridotites ( Mid-Atlantic Ridge , 15 ° 20 ′ N , ODP Leg 209 ): Implications for fluid / rock interaction in slow spreading environments. Chem. Geol. 234, 179–210. https://doi.org/10.1016/j.chemgeo.2006.04.011

Peach, B.N., Horne, J., Gunn, A.G., Clough, C.T., 1907. The Geological Structure of the North-West Highlands, in: Memoir of the Geological Survey of Great Britain.

Power, M.R., Pirrie, D., Andersen, J.C., Butcher, A.R., 2000. Stratigraphic distribution of platinum-group minerals in the Eastern Layered Series, Rum, Scotland. Miner. Depos. 35, 762–775.

https://doi.org/10.1007/s001260050278

Rollinson, H., 2007. Recognising early Archaean mantle : a reappraisal. Contrib. to Mineral. Petrol. 154, 241–252. https://doi.org/10.1007/s00410-007-0191-y

Rollinson, H., Gravestock, P., 2012. The trace element geochemistry of clinopyroxenes from pyroxenites in the Lewisian of NW Scotland: Insights into light rare earth element mobility during granulite facies metamorphism. Contrib. to Mineral. Petrol. 163, 319–335. https://doi.org/10.1007/s00410-011-0674-8

Rollinson, H.R., Windley, B.F., 1980. An archaean granulite-grade tonalite-trondhjemite-granite suite from scourie, NW Scotland: Geochemistry and origin. Contrib. to Mineral. Petrol. 72, 265–281. https://doi.org/10.1007/BF00376145

Sheraton, J.W., Skinner, A.C., Tarney, J., 1973. The geochemistry of the Scourian gneisses of the Assynt district, in: The Early Precambrian Rocks of Scotland and Related Rocks of Greenland. University of Keele, pp. 13–30.

Sills, J.D., 1981. Geochemical studies of the Lewisian Complex of the western Assynt region, NW Scotland. University of Leicester.

Smithies, R.H., Ivanic, T.J., Lowrey, J.R., Morris, P.A., Barnes, S.J., Wyche, S., Lu, Y., 2018. Two distinct origins for Archean greenstone belts. Earth Planet. Sci. Lett. 487, 106–116.

Sutton, J., Watson, J.V., 1951. The pre-Torridonian metamorphic history of the Loch Torridon and Scourie areas in the northwest Highland, and its bearing on the chronological classification of the Lewisian. Q. J. Geol. Soc. 106, 241–307.

Szilas, K., Kelemen, P.B., Bernstein, S., 2015. Peridotite enclaves hosted by Mesoarchaean TTG-suite orthogneisses in the Fiskefjord region of southern West Greenland. GeoResJ 7, 22–34. https://doi.org/10.1016/j.grj.2015.03.003

Szilas, K., van Hinsberg, V., Mcdonald, I., Næraa, T., Rollinson, H., Adetunji, J., Bird, D., Hinsberg, V. Van, Mcdonald, I., Næraa, T., Rollinson, H., Adetunji, J., Bird, D., 2018. Highly refractory Archaean peridotite cumulates: Petrology and geochemistry of the Seqi Ultramafic Complex, SW Greenland. Geosci. Front. 9, 689–714. https://doi.org/10.1016/j.gsf.2017.05.003

Taylor, R.J.M., Johnson, T.E., Clark, C., Harrison, R.J., 2020. Persistence of melt-bearing Archean lower crust for > 200 m.y.— An example from the Lewisian Complex , northwest Scotland. Geology 48. https://doi.org/10.1130/G46834.1/4906652/g46834.pdf

Van Kranendonk, M.J., Collins, W.J., Hickman, A., Pawley, M.J., 2004. Critical tests of vertical vs. horizontal tectonic models for the Archaean East Pilbara Granite-Greenstone Terrane, Pilbara Craton, Western Australia. Precambrian Res. 131, 173–211. https://doi.org/10.1016/j.precamres.2003.12.015

Weaver, B.L., Tarney, J., 1981. The Scourie Dyke Suite: petrogenesis and geochemical nature of the Proterozoic sub-continental mantle. Contrib. to Mineral. Petrol. 78, 175–188.

Wheeler, J., Park, R.G., Rollinson, H.R., Beach, A., 2010. The Lewisian Complex: insights into deep crustal evolution. Geol. Soc. London, Spec. Publ. 335, 51–79. https://doi.org/10.1144/SP335.4

Whitehouse, M.J., Fedo, C.M., 2003. Deformation features and critical field relationships of early Archaean rocks , Akilia , southwest Greenland. Precambrian Res. 126, 259–271. https://doi.org/10.1016/S0301-9268(03)00098-6

Whitehouse, M.J., Kemp, A.I.S., 2010. On the difficulty of assigning crustal residence, magmatic protolith and metamorphic ages to Lewisian granulites: constraints from combined in situ U-Pb and Lu-Hf isotopes. Geol. Soc. London, Spec. Publ. 335, 81–101. https://doi.org/10.1144/SP335.5